**Journal of Science and Technology in The Tropics**
Volume 13 Number 2 June 2017

# CONTENTS

# Prevalence and Characterization of Gastrointestinal Parasites Infection in Goats from Small-Scale Farms in Northern Part of Terengganu State, Peninsular Malaysia

**Lokman Mohd Azrul[1,2*], Che Razali Mohd Noor[2], Kanokporn Poungpong[3], Somkiert Prasanpanich[3] and Sathaporn Jittapalapong[4]**

[1]Animal Husbandry Laboratory, School of Food Science and Technology, Universiti Malaysia Terengganu, 21030, Kuala Terengganu, Terengganu, Malaysia
[2]Animal Health Division, Veterinary Services District Office, Bandar Permaisuri, 22100, Setiu, Terengganu, Malaysia
[2]Department of Animal Science, Faculty of Agriculture, Kasetsart University, Bangkhen Campus, 10900, Bangkok, Thailand
[3]Department of Parasitology, Faculty of Veterinary Medicine, Kasetsart University, Bangkhen Campus, 10900, Bangkok, Thailand
*Correspondence author email: azrullokman@umt.edu.my

*Received: 12-07-2017; accepted: 14-09-2017*

**Abstract** The objectives of this study were to observe the prevalence of gastrointestinal parasites in goats and to describe the infection characterization focusing on small-scale farms in Northern Terengganu**.** A total of 197 goats were involved in this study. Faecal samples were freshly collected for faecal egg count following Modified McMaster method. Total herd prevalence for this sampling area was 100% with 82.23% of individual infection. Among the infected goats, 67.28% were infected with mixed parasites. The rest were infected with single type of infection that 7.41% were only infected with helminth and 25.31% were only infected with protozoa. From positive samples, morphological of egg was used to identify the species involved including nematodes; Strongyle group (68.52%), *Strongyloides papillosus* (0.62%), *Trichuris* sp. (0.62%) and cestodes including *Moniezia expansa* (17.28%) and *Moniezia benedeni* (2.47%). Meanwhile for protozoa, three species were recorded including *Giardia* spp. cyst (7.41%), *Entamoeba* sp. (40.74%) and unsporulated coccidian oocyst, *Eimeria* spp. (55.55%). This prevalence study has confirmed the infection of gastrointestinal parasites from small-scale farms in this area and controlling methods is in need to be explained to the local farmers.

**Keywords** Prevalence – gastrointestinal parasites – modified McMaster method – goats – Terengganu state

## INTRODUCTION

Goat products; meat and milk are important elements as commodities for global livestock industry [1]. Meat and dairy products are consumed by people from all over the world [2]. The consistently increasing trend of human population in the world has resulted to additional need for animal products from time to time [3]. Same situation is also occurred in Malaysia

as local demand for goat meat and milk has been increased [4] due to the nutritional status compared to the products from other animals [5, 6].

Goat husbandry is important in improving economic status of local farmers. Due to this economic opportunity, farmers from many countries worldwide have been developed the interest for goat production including in Malaysia. According to the recent statistics, the population of goats in Malaysia in 2014 was nearly 500 thousand heads, showing increasing trend for 10 years whereas number of goats in 2004 was only 265 thousand heads [7]. Specifically in Terengganu, the population of goats in this state is among the highest in Malaysia, which is 35,294 heads in 2013. As a comparison with other states in east coast of Peninsular Malaysia, goats' number in Terengganu is slightly same with neighboring states; Pahang (35,772 heads), but lower than Kelantan (40,145 heads) [8].

While expanding the goat industry, a range of diseases, which resulted in goats' mortality and morbidity, has been negatively affected goat production [9-11]. Gastrointestinal parasites infection is a serious problem worldwide including in Malaysia which can affect the production and economic profit [12] due to slow growth rate of young animals and adverse effect on the performance of adult animals [13-15]. The effects of parasitic infection can cause death and these effects are likely to be a significant limitation for goats' productivity in Malaysia [16].

Gastrointestinal parasites infections in Malaysia have been reported previously with most of the studies were focusing on state level. For record, studies were conducted in few states mostly in west coast of Peninsular Malaysia namely Perak [17-19], Penang [20] and Selangor [21] and there was a study conducted generally in Peninsular Malaysia [22]. For Terengganu state, there were two recent reports on prevalence study with limited scope due to the number of farms involved and studies were mainly discussed about the intensity of the prevalence between two farms in one district [23] and within three farms in three districts [24].

Therefore, this study was conducted to provide the prevalence assessment of gastrointestinal parasites infection in Terengganu with more number of farms involved within northern districts in Terengganu compared to previous reports. Characterization of the infection and group of parasites were also presented.

## MATERIALS AND METHODS

### Study area

Study was conducted for a period of 2 months from November 2014 in northern part of Terengganu state, located at east coast of Peninsular Malaysia. A total of 16 small-scale farms (n=16) in 5 different districts namely Kuala Terengganu, Hulu Terengganu, Kuala Nerus, Setiu and Besut were involved as suggested by the authority of the Department of Veterinary Services (DVS) of Terengganu. Only small-scale farms with not more than 50 animals per farm were randomly selected for this study. This is due to the intention to observe the concern of local farmers regarding the usage of anthelmintic drugs and gastrointestinal parasitic diseases in goats.

**Animal samples**

Total number of 197 goats consisted of meat (crossbred of Boer and Katjang) and dairy (Saanen) were involved. From total sample, 77.16% (n=152) were females and the rest were males (n=45). The animals involved were aged not more than 24 months old.

**Faecal sample collection**

Faecal samples were freshly collected from goats' rectum using sterile disposable plastic glove. Faecal collection was conducted in the morning from 0900 to 1200 sampling time. Each sample was directly placed in a separate plastic bag, labeled and packed in a cooler box before stored at 4$^{o}$C pending for analysis [25].

**Faecal sample examination**

Faecal samples were examined at the Animal Husbandry Laboratory, School of Food Science and Technology, Universiti Malaysia Terengganu. Modified McMaster method was conducted for each sample to examine parasites eggs and cysts. Briefly, 3 g of faeces were mixed with saturated salt (NaCl) solution. After mixed vigorously, a sample of the mixture was taken with a pipette and was transferred to one of the chambers of the McMaster slide. This procedure was repeated and the other chamber was filled up. After 30 sec, total number of eggs under both of the etched areas on the slide was counted. The eggs were floated just below the top of the chamber. The total number of eggs in two chambers was multiplied by 100 eggs to get the egg per gram (EPG) value. Each egg, which detected under microscope was classified into groups of parasites based on its morphological characteristics [25, 26].

**Statistical analysis**

The overall data were analyzed using descriptive statistics. Prevalence of infection was determined both at herd and individual levels at 95% confidence interval (CI).

## RESULTS

Total numbers of 197 faecal samples from 16 small-scale farms were examined. All farms had at least three infected goats with gastrointestinal parasites, either mixed or single infection. Therefore, herd prevalence for this sampling area was 100% (95% CI, 69.4 – 73.3). For individual prevalence, 162 animals were infected. Thus, the infection prevalence for individual was 82.23% (95% CI, 61.08 – 76.22) and 17.77% of the animals were not infected. Among those infected animals, 67.28% were infected with mixed parasites. The rest were infected with single type of parasites which 7.41% only infected with helminth and 25.31% only infected with protozoa (Table 1). Helminths observed for these samples were divided into nematode and cestode while there was no trematode detected from infected animals. Infection was also reported by parasites group which 48.03% were infected with more than one group of parasites while the rest 51.97% were only infected by single group (Table 2).

Based on the morphological characteristics, eggs and cyst of gastrointestinal parasites were classified. From 162 positive samples, parasites detected were nematode, cestode and

protozoa. For helminths, nematodes observed including Strongyle group (68.52%), *Strongyloides papillosus* (0.62%) and *Trichuris* sp. (0.62%), while for cestodes, it's including *Moniezia expansa* (17.28%) and *Moniezia benedeni* (2.47%). Meanwhile for protozoa, species found were *Giardia* spp. (7.41%), *Entamoeba* sp. (40.74%) and unsporulated coccidian oocyst, *Eimeria* spp. (55.55%) (Table 3).

**Table 1.** Characteristic for individual infection

| Characteristic of infection | Number of samples (%) |
|---|---|
| Negative infection | 35 (17.77)[a] |
| Positive infection | 162 (82.23)[a] |
| Mixed infection of helminth and protozoa | 109 (67.28)[b] |
| Single infection of helminth | 12 (7.41)[b] |
| Single infection of protozoa | 41 (25.31)[b] |

[a]Percentage out of total animals, n = 197
[b]Percentage out of infected animals, n = 162

**Table 2.** Characteristic of infection based on parasites groups

| Characteristic of infection by parasites groups | Number of samples (%)[a] |
|---|---|
| **Infection by more than one group of parasites** | |
| Infected with protozoa + nematodes + cestodes | 18 (11.11) |
| Infected with protozoa + nematodes | 82 (50.62) |
| Infected with protozoa + trematodes | 0 |
| Infected with protozoa + cestodes | 9 (5.56) |
| Infected with nematodes + cestodes | 1 (0.62) |
| **Infection by single group of parasites** | |
| Infected only by nematodes | 10 (6.17) |
| Infected only by trematodes | 0 |
| Infected only by cestodes | 1 (0.62) |
| Infected only by protozoa | 41 (25.31) |

[a]Percentage out of infected animals, n=162

## DISCUSSION

The total 100% herd prevalence observed in this study denotes that gastrointestinal parasites infection is a widespread problem in northern part of Terengganu. This is a common findings as it also observed in previous reports conducted in Terengganu [23, 24] despite those studies were conducted in different type of farms (commercial farms) and total number of farms and animals involved.

**Table 3.** Parasites classification, stages observed and percentage out of infected animals

| Parasites | Stage observed | Number of samples (%)[a] |
|---|---|---|
| **Nematodes** | | |
| Strongyle group | Egg | 111 (68.52) |
| *Strongyloides papillosus* | Egg | 1 (0.62) |
| *Trichuris* sp. | Egg | 1 (0.62) |
| **Cestodes** | | |
| *Moniezia expansa* | Egg | 28 (17.28) |
| *Moniezia benedeni* | Egg | 4 (2.47) |
| **Protozoa** | | |
| *Eimeria* spp. | Oocyst | 90 (55.55) |
| *Entamoeba* spp. | Cyst | 48 (40.74) |
| *Giardia* spp. | Cyst | 12 (7.41) |

[a]Percentage out of infected animals, n = 162

Total numbers of 197 faecal samples from 16 small-scale farms were examined for coprological test. All farms had at least three goats infected with gastrointestinal parasites either mixed or single infection. Therefore, herd prevalence for this sampling area was 100% (95% CI, 69.4 – 73.3). For individual prevalence, 162 animals were infected. Thus, the infection prevalence for individual was recorded at 82.23% (95% CI, 61.08 – 76.22) and 17.77% of the animals was not infected. Among those infected animals, 67.28% were infected with mixed parasites. The rest were infected with single type of parasites which 7.41% infection only with helminths and 25.31% only infected with protozoa (Table 1).

Helminths observed for these samples were divided into nematode and cestode while there was no trematode detected from infected animals. Infection was also reported by parasites group which 48.03% were infected with more than one group of parasites while the rest 51.97% were only infected by single group of parasites (Table 2).

As a comparison for individual prevalence with another report in Terengganu case [26], individual prevalence reported in this study was higher for both helminth and protozoa

infection. Report by [24] stated that infection rates of helminth and protozoa for sample group in three districts in Terengganu were 77.7% and 89.2%, respectively, while for this study, infection rates were 89.51% and 92.59%, appropriately. This significant difference results might due to the type of farms involved which only small-scale farms with no anthelmintic usage history were chosen for this study ($P<0.05$), whereas commercial farms with proper management were used as a sample group in previous report. Both reports by [23] and [24] stated that goats were exposed for grazing during the day and kept in animal house at night. For this study, due to limited area for grazing, some of the farmers still need to proceed with cut and carry system for the forage after grazing time. Wet grasses with parasites eggs also can be a reason for high prevalence of gastrointestinal parasites as discussed before in previous studies conducted in rainy and wet season with wet grasses fed to the animals [27, 28]. Another reason for higher prevalence in this study is the environmental aspect. Sampling work for this study was conducted at the end of the year (November to December) that recorded highest rainfall in Terengganu as high as 800mm [29].

Based on the eggs morphological characteristics, strongyle group is the most dominant species in this current study with 68.52% prevalence of infection. From morphological differentiation under microscopic examination, two types of strongyle; *Haemonchus contortus* and *Trichostrongylus colubriformis* were found from the positive samples. Nevertheless, there was no distinctly density for prevalence for these two species in this study as all strongyle eggs were only categorized as the same group. This is in agreement with previous studies, which reported that these two species are the most important for infection problem in ruminants worldwide as same as reported in studies in few states in Peninsular Malaysia [17-22]. Another nematodes found in this study were *Strongyloides papillosus* or threadworm and *Trichuris* sp. or whipworm, both at the very low population with same prevalence (0.62%). Prevalence of *S. papillosus* was higher in previous reports [23, 24]. This nematode is capable in penetrating the skin of the host, making prevalence of this species high in freely grazing animals [30]. *Trichuris* sp. infection was recorded at low density in this study and previous reports as infection with this whipworm is not common but can be found mainly in early age of goats [31]. Thus, sample group dominated with young animals have a potential with high *Trichuris* sp. infection [31].

There was no trematode detected in this study. For cestode, two species of tapeworm namely *Moniezia expansa* and *Moniezia benedeni* were detected with low prevalence, 17.28% and 2.47%, respectively. Tapeworm eggs were common in goats as reported in necropsy study of the goats conducted in University Veterinary Hospital (UVH) of Universiti Putra Malaysia (UPM) where half of the total samples of goats (n=72) were infected with tapeworm [32]. Meanwhile, the unsporulated coccidian, *Eimeria* spp. oocyst was the most common protozoa species found (55.55%) within this sample group. Another two protozoan species were also observed, *Entamoeba* sp. (40.74%) and *Giardia* sp. (7.41%). All three species are familiar for protozoan infection [21, 24].

## CONCLUSION

This study concludes that gastrointestinal parasites infection is widespread in northern part of Terengganu. Characteristic of farms with different grazing management and anthelmintic history might be the reason for different density for prevalence data. Further studies on analysis of farm management and controlling parasites infection in this sampling area should be conducted in the future.

**Acknowledgement –** This work is funded by Ministry of Higher Education (MoHE) of Malaysia for financial support under the research budget for 'Skim Latihan Akademik Bumiputra' for young academician. A million thanks to the staff of Veterinary Services District Office, Department of Veterinary Services (DVS) Terengganu for helping during fieldworks and laboratory staff at Universiti Malaysia Terengganu (UMT) for technical support. Thanks to Dr. Khadijah Saad of UMT for research discussion and also thanks to the local farmers for their involvement in this study.

## REFERENCES

1. Copland J.W. (1984) *Goat production and research in the tropics*: In: The Proceeding of a Workshop held at the University of Queensland, Brisbane, Australia. ACIAR Proceedings Series No. **7**, p. 118.
2. Thornton P.K. (2010) Livestock production: recent trends, future prospects. *Philosophical Transactions of the Royal Society B* **365**: 2853-2867.
3. Hoste H. and Torres-Acosta J.F.J. (2011) Non-chemical control of helminths in ruminants: Adapting solutions for changing worms in a changing world. *Veterinary Parasitology* **180**: 144-154.
4. Kaur B. (2010) Consumer preference for goat meat in Malaysia: Market opportunities and potential. *Journal of Agribusiness Market* **3**: 40-55.
5. Casey N.H. (1992) *Goat meat in human nutrition*. In: The Proceedings of V International Conference on Goats. Indian Council of Agricultural Research, New Delhi.
6. Correa JE (2016). *Nutritive value of goat meat*. The Alabama Cooperative Extension System, Alabama A&M University and Auburn University. From http://www.aces.edu/pubs/docs/U/UNP-0061/UNP-0061.pdf [Retrieved August 19th 2016].
7. FAO (2016). *Number of heads of goats in selected country (Malaysia) 2004 – 2014*. Food and Agriculture Organization of the United Nation, Statistic Division. From http://faostat3.fao.org/browse/Q/QA/E [Retrieved on August 19th 2016].
8. DVS (2014). *Selected indicators for agriculture, crops and livestock, Malaysia 2014*. Department of Veterinary Services of Malaysia. From https://www.statistics.gov.my/portaL_@Old/download_Agriculture/files/Selected_Agricultural_Indicators_Malaysia_2014.pdf [Retrieved on August 20th 2016].
9. Sykes A.R. (1994) Parasitism and production in farm animals. *Animal Production* **59**: 155-172.

10. Waller P.J. (1999) International approaches to the concept of integrated control of nematode parasites of livestock. *International Journal of Parasitol*ogy **29**: 155-164.
11. Sani R.A. and Gray G.D. (2004) *Worm control for small ruminants in South East Asia*. In: Sani R.A., Gray G.D. and Baker R.L. (eds.) Worm control for small ruminants in Tropical Asia. ACIAR Monograph **113**, p. 3-21.
12. Fadzil M.Y. (1977) *The economic importance of parasitism in food animals in Peninsular Malaysia*. In: The Proceedings of the Conference on Health and Production of Local and Australian Cattle in Southeast Asia. Kuala Lumpur, p. 62-79.
13. Kochapakdee S., Choldumrongkul S., Saithanoo S. and Pralomkarn W. (1993) *The effects of internal parasites on growth of crossbred goats under village environment in Southern Thailand: Advance in sustainable animal ruminant-tree cropping integrated systems.* In: The Proceedings of a Workshop University of Malaya, Kuala Lumpur, p. 198-202.
14. Pralomkarn W., Saithanoo S., Ngampongsai W., Suwanrut C. and Milton J.T.B. (1996) Growth and puberty traits of Thai Native (TN) and TN x Anglo-Nubian does. *Asian-Australasian Journal of Animal Science* **9**: 591-595.
15. Apichartsarangkool T., Sriphai A., Thonglorm S. and Sriwichai Y. (2003) Treatment results of goats and sheep infected with gastrointestinal nematode. *Journal of Agriculture* **19**: 86-92.
16. Symoens C., Dorny P., Alimon R., Jalila A., Hardouin J. and Vercruysse J. (1993) *Productivity of goats in smallholdings of Peninsular Malaysia*. In: The Proceedings of the Workshop on Development of Sustainable Integrated Small Rminants – Tree Cropping Production Systems. University of Malaya, Kuala Lumpur, p. 129-136.
17. Chandrawathani P., Nurulaini R., Adnan M., Premalaatha B., Khadijah S., Jamnah O., et al. (2009) A survey of parasitic infection on small ruminant farms in Kinta and Hilir Perak Districts, Perak, Malaysia. *Tropical Biomedicine* **26:** 11-15.
18. Norakmar I., Chandrawathani P., Nurulaini R., Zawida Z., Premaalatha B., Imelda Lynn V., Adnan M., Jamnah O. and Zaini, C.M. (2010) Prevalence of helminthiasis in relation to climate in small ruminants in Perak in 1998 and 2008. *Malaysian Journal of Veterinary Research* **1**(1): 37-44.
19. Zainalabidin F.A., Raimy N., Yaacob M.H., Musbah A., Bathmanaban P., Ismail E.A., et al. (2015) The prevalence of parasitic infection of small ruminant farms in Perak, Malaysia. *Tropical Life Sciences Research* **26**: 1-8.
20. Wahab A.R. and Adanan C.R. (1992) Observations on the worms egg counts and their nematode species in goats from the North-East District of Penang Island, Peninsular Malaysia. *Pertanika* **15**: 221-224.
21. Jalila A., Dorny P., Sani A.R., Salim N.B. and Vercruysse J. (1998) Coccidial infections of goats in Selangor, Peninsular Malaysia. *Veterinary Parasitology* **74**: 165-172.
22. Dorny P., Symoens C., Jalila A., Vercruysse J. and Sani A.R. (1995) Strongyle infections in sheep and goats under the traditional husbandry system in Peninsular Malaysia. *Veterinary Parasitology* **56**: 121-136.
23. Khadijah S., Andy T.F.H., Khadijah S.S.A.K., Khairi A.K.M., Nur Aida, H. and Wahab A.R. (2014) Parasites infection in two goat farms located in Kuala Terengganu, Peninsular Malaysia. *Asian Journal of Agriculture and Food Science* **2**: 463-468.

24. Yusuf A.M. and Md Isa M.L. (2016) Prevalence of gastrointestinal nematodiasis and coccidiosis in goats from three selected farms in Terengganu, Malaysia. *Asian Pacific Journal of Tropical Biomedicine*, doi: 10.1016/j.apjtb.2016.07.001.
25. Christopher R., Chandrawathani P. and Cheah T.S. (1992) *Manual on Parasitology*. In: Loganathan P. (ed.) Department of Veterinary Services, Malaysia, p. 12-14.
26. MAFF (1986) *Manual of Veterinary Parasitological Laboratory Techniques*. Ministry of Agriculture, Fisheries and Food of United Kingdom, Her Majesty's Stationary Office, London.
27. Rahman M.A., Sharifuzzaman M., Khokon, J.U., Sarker E.H., Shahiduzzaman M. and Mostofa M. (2014). Prevalence of parasitic diseases of goats at Pirganj upazilla at Bangladesh. *International Journal of Natural and Social Science* **1**: 8-12.
28. Zvinorova P.I., Halimani T.E., Muchadeyi F.C., Matika O., Riggio V. and Dzama K. (2016). Prevalence and risk factors of gastrointestinal parasitic infections in goats in low-input low-output farming systems in Zimbabwe. *Small Ruminant Research* **143**: 75–83.
29. METMalaysia (2016). *Ringkasan Hujan Bulanan Terkini*. Jabatan Meteorologi Malaysia (METMalaysia) (In Malay) From http://www.met.gov.my/ web/ metmalaysia/ climate/ climatechange/ climateinformation/ monthlyrainfallreview [Retrieved on August 21st 2016].
30. Chandrawathani P., Omar J. and Waller P.J. (1998) The control of the free-living stages of *Strongyloides papillosus* by the nematophagous fungus *Arthrobotrys oligospora*. *Veterinary Parasitology* **76:** 321-325.
31. Fox MT (2014). Gastrointestinal parasites of sheep and goats. From http://merckvetmanual.com [Retrieved on August 21st 2016].
32. Sani R.A., Adnan M., Cheah T.S. and Chandrawathani P. (2004) Worm control for small ruminants in Serdang, West Malaysia. *Kajian Veterinar* **17**: 127-131.

*Journal of Science and Technology in the Tropics* (2017) 13(2): 63-74

# Pulsed Electric Field Exposed HeLa Cells Alignment on Extracellular Matrix Protein Patterned Surface

Muhammad Mahadi Abdul Jamil[1*], Mohamed A. Milad Zaltum[1] and Morgan C. T. Denyer[1,2]

[1]*Biomedical Modeling and Simulation (BIOMEMS) Research Group, Department of Electronic Engineering, Faculty of Electrical and Electronics Engineering,*
*University Tun Hussein Onn Malaysia, 86400 Parit Raja, Batu Pahat, Johor, Malaysia*
[2]*Faculty of Life Sciences, University of Bradford, University of Bradford, Yorkshire, BD7 1DP, UK*
*Correspondence author email: mahadi@uthm.edu.my

*Received: 12-07-2017; accepted:14-09-2017*

**Abstract**
Cell behavior in terms of adhesion, orientation and guidance, on extracellular matrix (ECM) molecules including collagen, fibronectin and laminin can be examined using micro contact printing (MCP). These cell adhesion proteins can direct cellular adhesion, migration, differentiation and network formation *in-vitro*. This study investigates the effect of micro-contact printed ECM protein, namely fibronectin, on alignment and morphology of HeLa cells cultured *in-vitro*. Fibronectin was stamped on plain glass cover slips to create patterns of 25 µm, 50 µm and 100 µm width. However, HeLa cells seeded on 50 µm induced the best alignment on fibronectin pattern (7.66° ±1.55SD). As a consequence of this, 50µm wide fibronectin pattern was used to see how fibronectin induced cell guidance of HeLa cells was influenced by 100 µs and single pulse electric fields (PEF) of 1kV/cm. The results indicates that cells aligned more under pulse electric field exposure (2.33° ± 1.52 SD) on fibronectin pattern substrate. Thus, PEF usage on biological cells would appear to enhance cell surface attachment and cell guidance. Understanding this further may have applications in enhancing tissue graft generation and potentially wound repair.

**Keywords:** HeLa cells alignment; Pulsed electric field; Micro contact printing; Extra cellular matrix

## INTRODUCTION

Micro-contact printing (MCP) is a technique that allows a surface to be readily functionalised with a material such as an extra cellular matrix (ECM) protein, in a defined pattern (Sefat *et al.,* 2011; Ricoult *et al.,* 2012; Berends *et al.,* 2009; Khaghani *et al.,* 2008). These cellular behaviours can then be used to interpret the cell signaling pathways related with the control of cell surface interactions (Kumar *et al.,* 1995; Kleinman *et al.,* 1990). Fibronectin is a transmembranous glycoprotein that exists in its soluble form in plasma. Its insoluble form can be found in connective tissue and the basal lamina (Pankov *et al.,* 2002). Fibronectin binds to collagen, fibrin, fibroblasts in the ECM and the plasma membrane of the cells, and it is a high

molecular weight protein. This protein plays a vital role in cell adhesion and re-organiation of the ECM (Carter, 1967; Salber *et al.,* 2007). The connection between cells and the ECM is also mediated by fibronectin. Fibronectin is a dimeric glycoprotein, comprised immers, each of approximately 250,000 molecular weight. Each of these subunits is folded three times (FN1, FN2, FN3) and contain the amino acid repeat FN1, FN2, FN3. Fibronectin can bind to collagen at the FN1/2 region, while the FN3 region takes up contact with the respective cells (Abdul Jamil, M. M., 2007; Pankov *et al.,* 2002). Alternative splicing forms completely different kinds of fibronectin. For example, the liver builds fibronectin that circulates as a dissolved element of the serum. However, static fibronectin is also formed in various tissues (Pankov *et al.,* 2002).

In natural skeletal tissues, the cells and the structures form spatial and oriented geometries and patterns (Zhu *et al.,* 2005). In recent research, significant work has been done to understand cell surface interaction and cell guidance for biomedical applications (Feinberg, 2008; Hamilton *et al.,* 2006). The potential applications of such biomedical systems include the micro-textures that helps in enhancing tissue integration and wound healing (Dalby *et al.,* 2003; Khang *et al.,* 2006; Berends *et al.,* 2009; Khaghani *et al.,* 2008). On the other hand, various polymer and metal materials have been commercially introduced. These materials often show poor and uncontrolled interactions with proteins and cells. This makes them difficult to integrate into the body tissues. To increase the bioactivity and biocompatibility, efforts have been made to deposit bioactive coatings onto implant surfaces. Contact guidance can be promoted by the use of chemical guidance cues (Folch *et al.,* 1998; Clark *et al.,* 1990). This is a phenomenon, which includes the alignment of cells, as they spread across micro-patterns. Another researcher (Su *et al.,* 2007) observed the effects of micro-patterned geometries on cell alignment. In microfluidic devices, BioMEMS and lab-on-a-chip applications, Polydimethylsiloxane (PDMS) has been widely used (Whitesides *et al.,* 2006; Cecchini *et al.,* 2008; Yea *et al.,* 2006) largely because of its biocompatibility and mechanical properties (Peterson *et al.,* 2005; Griscom *et al.,* 2002). Researchers have also analyzed the effects of micro-patterning on cell spreading and alignment on PDMS (Chaw *et al.,* 2007; Salber *et al.,* 2007).

Formation of detailed surface patterns on glass, polymer or metal materials could allow further clarification about the factors that control cell adhesion, cell proliferation, differentiation and molecular signaling pathways on material surfaces (Ogaki *et al.,* 2010; Diener *et al.,* 2005). These surface-engineered materials are expected to be able to control the shape, size cell/cell coupling of the attached cells during guided network formation.

The aims of this study are to characterize HeLa cell guidance on micro contact printed fibronectin patterns, and to then determine how that guidance is modified by pulse electric field.

## MATERIALS AND METHODS

### *Cell culture*

In this study, HeLa cells were cultured in RPMI-1640 medium supplemented with 10% fetal bovine serum (FBS) and 1% penicillin-streptomycin at 37˚C in a 5% humidified $CO_2$ incubator. When the HeLa cells reached 80 to 90% confluence, media was removed from the

tissue culture flask, then, 3ml of phosphate buffered saline (PBS) was added in the flask to wash the cells, which was removed after few seconds. About 2 ml of TryPle Express from GIBCO was added to detach the cells from bottom of the flask. TryPle Express works best in a warm surrounding, so the flask was incubated for seven minutes at 37°C. After detachment, the HeLa cells were counted by haemocytometer. Thereafter, 800µl of cells suspension at a concentration of $3.75\times10^4$ cell/ml (equivalent to 30,000 cells) were transferred into a 4 mm cuvette for electroporation.

***Stamp fabrication***

Master stamps (glass template) repeat gratings containing 25µm, 50µm and 100µm wide ridge (width) with 5µm deep channels at the University of Glasgow (Abdul Jamil *et al.*, 2008). PDMS stamps were formed at the University of Bradford from these templates. Firstly, the template was coated with 2% dimethylchlorosilane mixed with 98% trichloroethylene, which made the surface hydrophobic. After that, 9ml of sylgard (silicon-based elastomer gel) and 1ml of curing agent were mixed with the templates and left to cure overnight. Vacuum processing was done to eliminate any air bubbles. After curing, the sylgard gel was removed from the template, which enabled the generation of sylgard stamps showing a negative relief of the template to be formed. These stamps were then used in functionalizing plain glass slides and gold coated test substrates with various proteins. Figure 1 show images of the PDMS stamps for 25µm, 50µm and 100µm width.

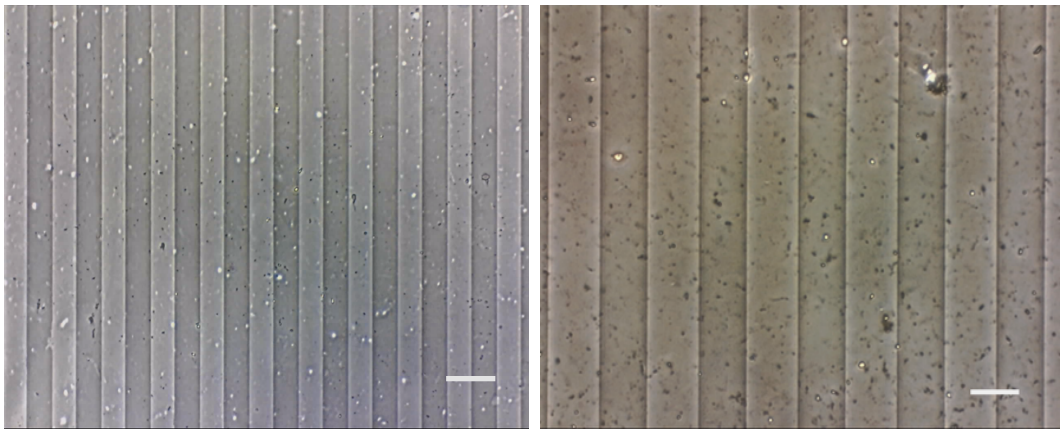

(a) 25 µm (b) 50 µm

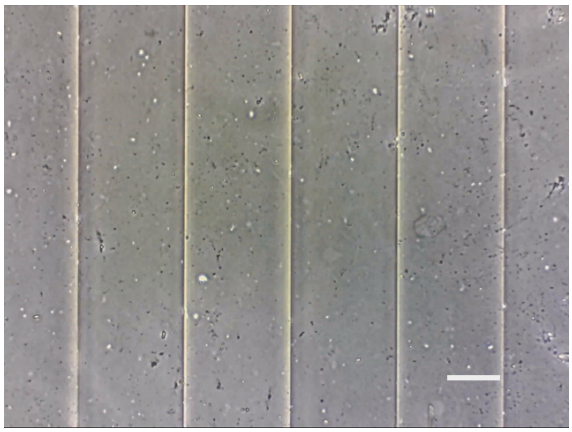

(c) 100 µm

Figure 1: PDMS stamps with (a) 25 µm, (b) 50 µm and (c) 100 µm width (scale bar 50 µm)

***Micro contact printing (MCP) technique***

All working environments (surfaces) before MCP, stamps and coverslips were sterilized with 70% ethanol and air dried in a laminar flow hood. After that plain glass coverslips were micro-contact printed with fibronectin. Inking the PDMS stamps was achieved by applying a 50µg/ml solution of fibronectin in PBS (Shen *et al.,* 2008) to the PDMS stamps for 60 minutes (Tan *et al.,* 2004; Khaghani *et al.,* 2008). Following inking the stamps were air-dried for 30 seconds. The stamps were then placed immediately in contact with the substrate and pressed slightly using another glass cover slip for 50 seconds (Abdul Jamil *et al.*, 2007). The same method was repeated for each stamp of the 25µm, 50µm and 100µm stamps. This allowed the substrate to be patterned with 25µm, 50µm and 100µm wide protein coated tracks, which are separated by 25µm, 50µm and 100µm wide uncoated tracks. Figure 2 demonstrates this process. MCP patterns were successfully transferred to the substrates. Though imperfections in the stamp and the use of manual pressure caused some differences in the track widths of the stamped protein.

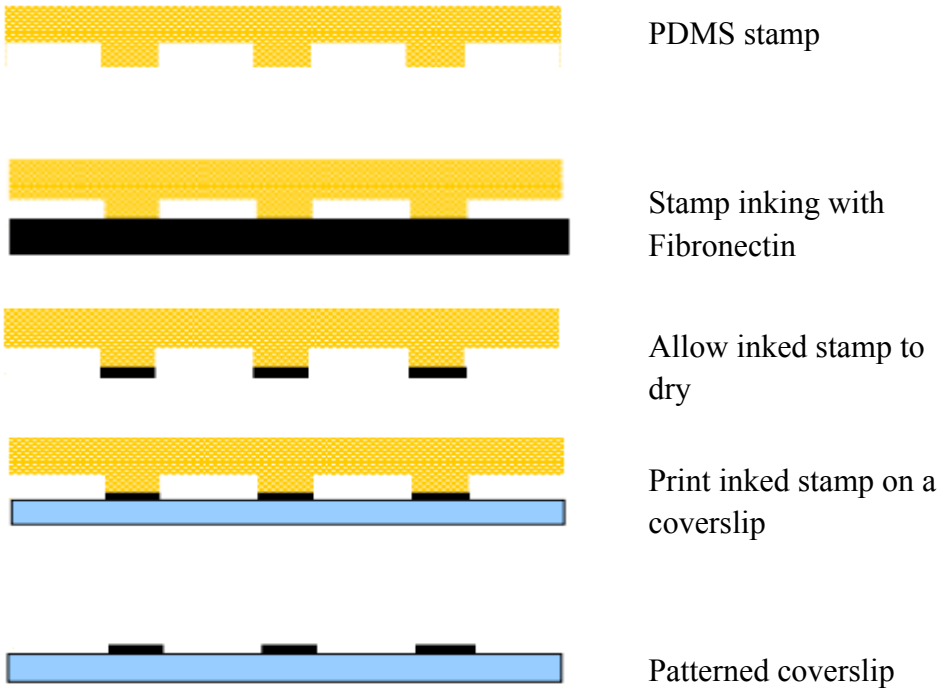


Figure 2: Illustration of the stamping process

***Cell Plating***

Plain glass slides and glass slides coated with un-patterned fibronectin were seeded with non-electroporated (NEP) HeLa cells at a concentration of 30,000 cells/coverslip for 18hrs as a control group. At the same time, glass slides with fibronectin micro-contact patterned printed with three different gratings (25µm, 50µm and 100µm widths) were also seeded with non-electroporated HeLa cells for 18hrs. After 18hrs, cells were then imaged with standard phase contrast light microscope. The pattern with better alignment was used for seeding electrically treated HeLa cells. This allowed the impact of single pulse electric fields on cell guidance to be determined by comparing cell guidance on the optimum fibronectin pattern with and without PEF treatment.

## RESULTS AND DISCUSSION

***Micro contact printing (MCP) technique***

The stamp consisted of ridges with 25 µm, 50 µm and 100 µm width fibronectin coated tracks separated by 25 µm, 50 µm and 100 µm width uncoated tracks. Micro-contact printing patterned of fibronectin on the cover glass (substrates) resulted in the substrates being successfully patterned with 25 µm, 50 µm and 100 µm width of repeated gratings as shown in Figure 3. The distances between the coated and uncoated channels have been marked by the yellow arrows.

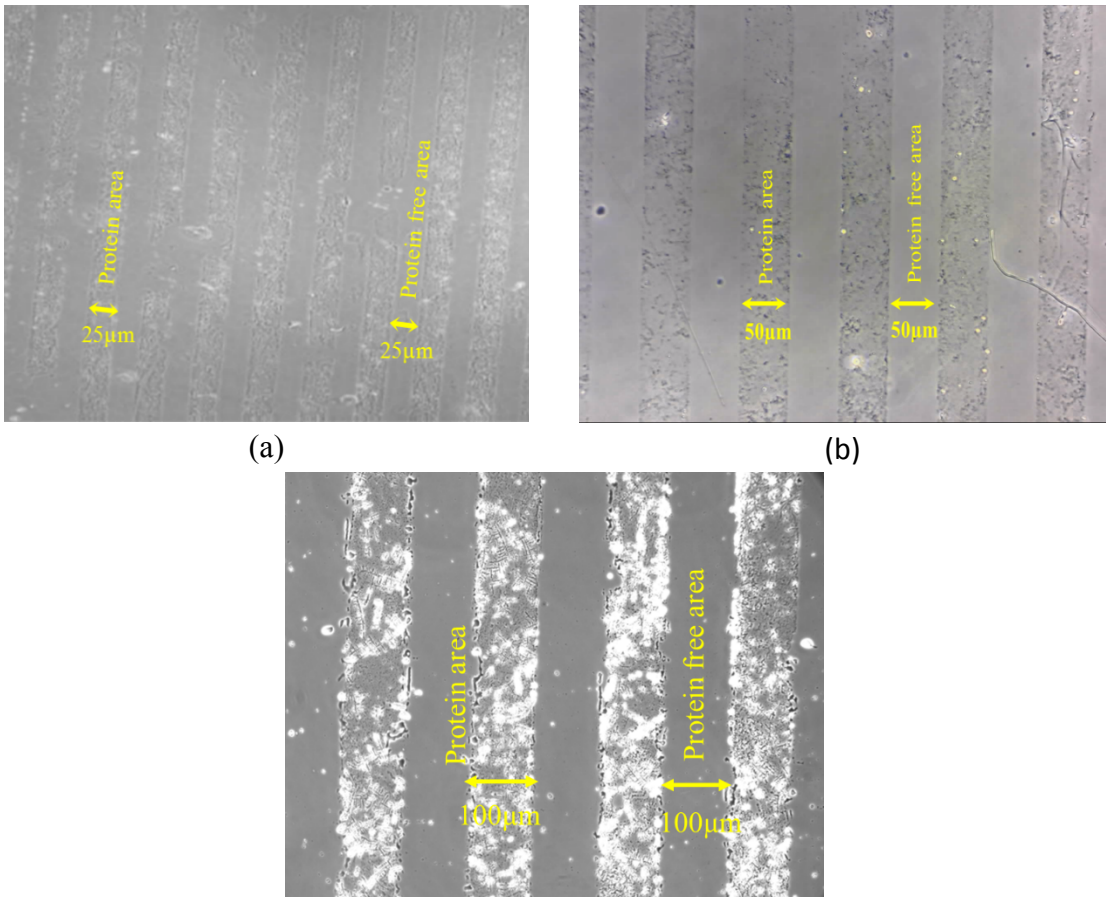


Figure 3: Actual images of (a) 25µm, (b) 50µm and (c) 100µm width protein patterns printed on glass coverslip

***Hela cells interactions with micro-patterned surface***

Substrate printed with chemical cues caused different cell responses like cell migration and cell alignment along the cues (Sefat *et al.,* 2011; Khaghani *et al.,* 2008; Su *et al.,* 2007). The effects of initial cell attachment on substrate were investigated by recording cell images up to 18hrs after cell culture using DinoCapture imaging software. After 18hrs in culture, the photomicrograph obtained from the plated HeLa cells showed different alignment to the MCP. It became clear that the HeLa cell seeded on uncoated and coated unpattern substrates (control group) did not show any alignment. This is obvious because even though coated, but there is no pattern for the cell to follow. Figure 4 shows the morphology of HeLa cells on the two control group substrates (uncoated and fibronectin-coated but unpattern substrates). Even though the control group are identical in terms of initial cell seeding density, passage number and incubator environment, they showed different morphology and adhesion capacity when compared with the pattern counterpart group. Most cells in the control group are rounded or rather more of an epithelial morphology ,which imply less adherence to the substrate (Sefat, 2013).

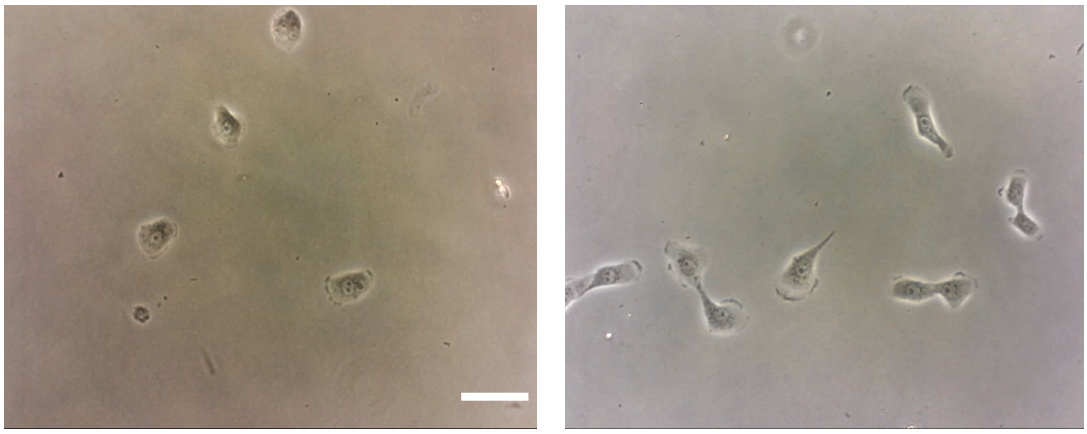

(a) Un-coated Sample without EP ›) Fibronectin coated Sample without EP

Figure 4: Photomicrographs of HeLa cells after 18hrs of seeding on (a) Un-coated coverslip glass, (b) Fibronectin coated on coverslip glass (control experiments) (scale bar 50µm)

However, the HeLa cells reacted differently to the various gratings of fibronectin patterned. HeLa cells seeded on 25µm patterned substrates induced a poor alignment (34° ±6.78SD). On the other hand, 50µm induced best alignment of the cells to the fibronectin pattern (7.66° ±1.55SD). Similarly, 100µm show good alignment (12.06° ±1.5SD) as compared to the 25µm pattern, but less than the 50µm pattern. As it shown in Figure 5, we can deduce that the fibronectin pattern substrate showed a better attachment with cells elongating along the pattern especially with the 50µm and 100µm, though more articulate with 50µm.

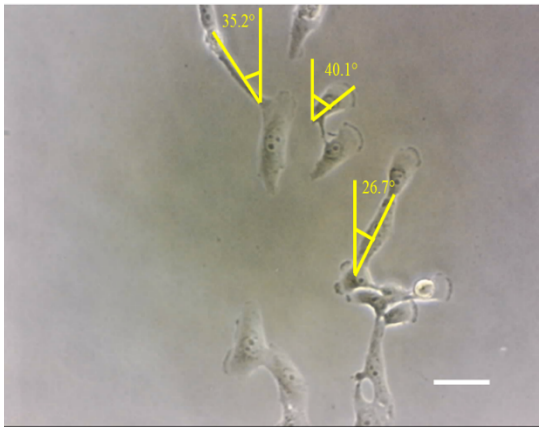


(a) 25µm micro contact printed of Fibronectin Sample

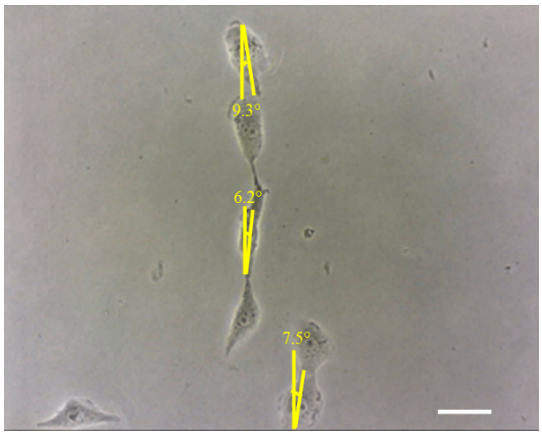


(b) 50µm micro contact printed of Fibronectin Sample

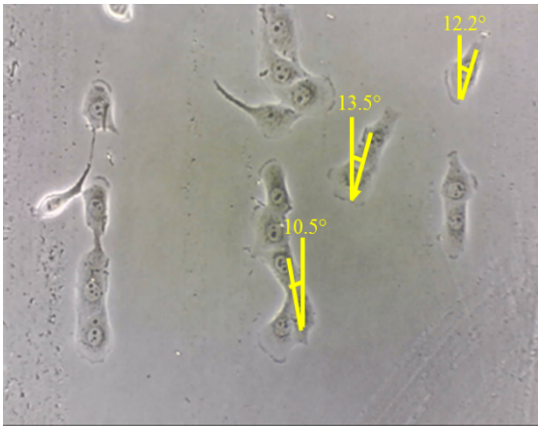


(c) 100µm micro contact printed of Fibronectin Sample

Figure 5: Photomicrographs of HeLa cells after 18hrs of seeding (a) 25µm, (b) 50µm and (c) 100µm micro contact printed of Fibronectin on coverslip glass (scale bar 50µm)

Furthermore, the 50µm that induced a better alignment was used to check the behavior of HeLa cells under the influence of electric field. Hence, the cells were electroporated (with 1kv/cm 100µs & single pulse) and seeded on to a 50µm fibronectin micro-patterned substrate and their morphology compared to the non-electroporated counterpart. The results as shown in Figure 6 indicates that cells were aligned (2.33° ±1.52SD) on fibronectin pattern substrate especially under pulse electric field exposure: with better alignment of the cells in the EP group (2.33° ±1.52SD), when compared to NEP group (7.66° ±1.55SD) on the same 50µm fibronectin patterned substrate.

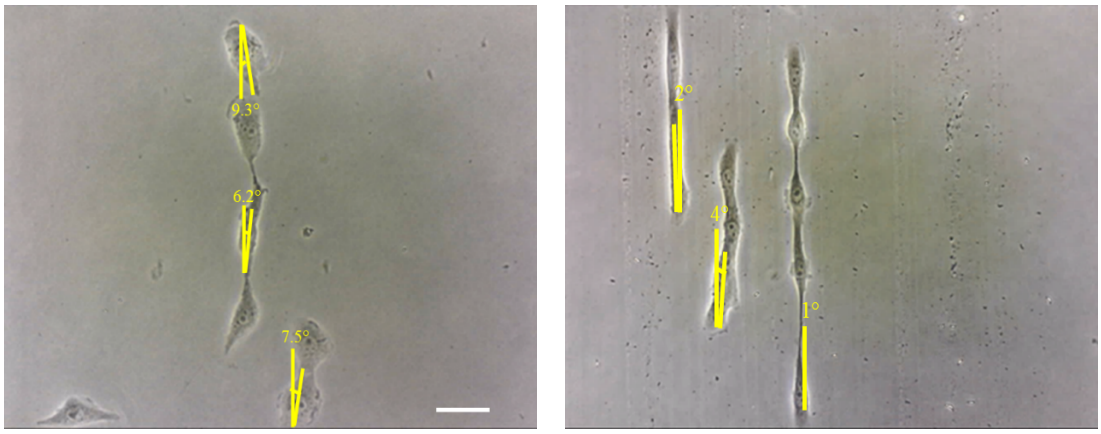


(a) 50µm micro contact printed of Fibronectin Sample without EP

(b) 50µm micro contact printed of Fibronectin Sample with EP

Figure 6: Photomicrographs of HeLa cells after 18hrs of seeding 50µm micro-contact printed of Fibronectin on coverslip glass (a) without EP and (b) with EP (scale bar 50µm)

This could indicate that the electric field stimulated a signaling pathway associated with enhancing cell adhesion, and hence increase the cell elongation and guidance (Mamman and Abdul Jamil, 2015). This finding is also in agreement to that of Zhang *et al.* (2011). Thus, the outcome of this study can be utilized in cell assembling and guidance of cells for wound healing application and tissue regeneration for implantation, for example antibody fluorescence based experiments to measure specific integrin up-regulation.

## CONCLUSION

The overall conclusion of this study is that PEF seems to enhance cell guidance on glass substrate micro-patterned with 50µm wide repeat gratings of fibronectin. This could indicate that in some way PEF and electroporation either modifies the distribution of fibronectin specific membrane bound integrins or results in their up, or down regulation. The manipulation of both may have implications in the enhancement of engineered tissue grafts technologies.

## ACKNOWLEDGMENTS

The researchers would like to thank Ministry of Higher Education Malaysia for the research grant under the Fundamental Research Grant Scheme (FRGS) phase 2/2014, Vot 1488, for supporting the research work.

## REFERENCES

Abdul Jamil, M. M. (2007). Application of a novel high resolution widefield surface plasmon microscope in cell engineering, wound healing and development of new

binding assays. PhD thesis submitted to the University of Bradford.

Abdul Jamil, M. M., Youseffi, M., Twigg, P. C., Britland, S. T., Liu, S., See, C. W., & Denyer, M. C. (2008). High resolution imaging of bio-molecular binding studies using a widefield surface plasmon microscope. Sensors and Actuators B: Chemical, 129(2), 566-574.

Abdul Jamil, M. M., Youseffi, M., Britland, S.T., Liu, S., See, C.W., Somekh, M.G., Denyer, M.C.T. (2007). Widefield Surface Plasmon Resonance Microscope: A Novel Biosensor Study of Cell Attachment to Micropatterned Substrates. 3rd Kuala Lumpur International Conference on Biomedical Engineering, Biomed, 15, 334-337.

Berends, R. F., Youseffi, M., Sefat, F., Khaghani, S. A., & Denyer, M. (2009). Investigating keratinocyte cell responses to ECM proteins using Microcontact printing. In Journal of Anatomy Vol. 215, No. 6, pp. 711-711.

Carter, S. B. (1967). Haptotactic islands: a method of confining single cells to study individual cell reactions and clone formation. Experimental cell research, 48(1), 189-193.

Cecchini, M., Girardo, S., Pisignano, D., Cingolani, R., & Beltram, F. (2008). Acoustic-counterflow microfluidics by surface acoustic waves. Applied Physics Letters, 92(10), 104103.

Chaw, K. C., Manimaran, M., Tay, F. E. H., & Swaminathan, S. (2007). Matrigel coated polydimethylsiloxane based microfluidic devices for studying metastatic and non-metastatic cancer cell invasion and migration.Biomedical microdevices, 9(4), 597-602.

Clark, P., Connolly, P., Curtis, A. S., Dow, J. A., & Wilkinson, C. D. (1990). Topographical control of cell behaviour: II. Multiple grooved substrata.Development, 108(4), 635-644.

Dalby, M. J., Riehle, M. O., Yarwood, S. J., Wilkinson, C. D., & Curtis, A. S. (2003). Nucleus alignment and cell signaling in fibroblasts: response to a micro-grooved topography. Experimental cell research, 284(2), 272-280.

Diener, A., Nebe, B., Lüthen, F., Becker, P., Beck, U., Neumann, H. G., & Rychly, J. (2005). Control of focal adhesion dynamics by material surface characteristics. Biomaterials, 26(4), 383-392.

Feinberg, A. W., Wilkerson, W. R., Seegert, C. A., Gibson, A. L., Hoipkemeier-Wilson, L., & Brennan, A. B. (2008). Systematic variation of microtopography, surface chemistry and elastic modulus and the state dependent effect on endothelial cell alignment. Journal of Biomedical Materials Research Part A, 86(2), 522-534.

Griscom, L., Degenaar, P., LePioufle, B., Tamiya, E., & Fujita, H. (2002). Techniques for patterning and guidance of primary culture neurons on micro-electrode arrays. Sensors and Actuators B: Chemical, 83(1), 15-21.

Hamilton, D. W., Wong, K. S., & Brunette, D. M. (2006). Microfabricated discontinuous-edge surface topographies influence osteoblast adhesion, migration, cytoskeletal organization, and proliferation and enhance matrix and mineral deposition in vitro. Calcified tissue international, 78(5), 314-325.

Khaghani, S., Sefat, F., Denyer, M., & Youseffi, M. (2008). Alignment of rat primary chondrocyte cells to collagen type-1, ficronectin and laminin. In Journal of

Anatomy Vol. 213, No. 3, pp. 351-351.

Khang, D., Sato, M., Price, R. L., Ribbe, A. E., & Webster, T. J. (2006). Selective adhesion and mineral deposition by osteoblasts on carbon nanofiber patterns. International journal of nanomedicine, 1(1), 65.

Kleinman, H. K., Sephel, G. C., TASHIRO, K. I., Weeks, B. S., Burrous, B. A., Adler, S. H., ... & Martin, G. R. (1990). Laminin in neuronal development.Annals of the New York Academy of Sciences, 580(1), 302-310.

Kumar, A., Abbott, N. L., Biebuyck, H. A., Kim, E., & Whitesides, G. M. (1995). Patterned self-assembled monolayers and meso-scale phenomena.Accounts of Chemical Research, 28(5), 219-226.

Mamman, H. B., & Jamil, M. M. (2015). Investigation of electroporation effect on HT29 cell lines adhesion properties. In Biomedical Engineering (ICoBE), 2015 2nd International Conference on (pp. 1-4). IEEE.

Ogaki, R., Alexander, M., & Kingshott, P. (2010). Chemical patterning in biointerface science. Materials today, 13(4), 22-35.

Pankov, R., & Yamada, K. M. (2002). Fibronectin at a glance. Journal of cell science, 115(20), 3861-3863.

Peterson, S. L., McDonald, A., Gourley, P. L., & Sasaki, D. Y. (2005). Poly (dimethylsiloxane) thin films as biocompatible coatings for microfluidic devices: cell culture and flow studies with glial cells. Journal of Biomedical Materials Research Part A, 72(1), 10-18.

Ricoult, S. G., Goldman, J. S., Stellwagen, D., Juncker, D., & Kennedy, T. E. (2012). Generation of microisland cultures using microcontact printing to pattern protein substrates. Journal of neuroscience methods, 208(1), 10-17.

Salber, J., Gräter, S., Harwardt, M., Hofmann, M., Klee, D., Dujic, J., & Groll, J. (2007). Influence of Different ECM Mimetic Peptide Sequences Embedded in a Nonfouling Environment on the Specific Adhesion of Human-Skin Keratinocytes and Fibroblasts on Deformable Substrates. Small, 3(6), 1023-1031.

Sefat, F. (2013). Cell engineering of human bone monolayers and the effect of growth factors and microcontact printed ECM proteins on wound healing. The role of ECM proteins, TGF¿-1, 2 and 3 and HCl/BSA in cellular adhesion, wound healing and imaging of the cell surface interface with the widefield surface plasmon microscope (Doctoral dissertation, University of Bradford).

Sefat, F., Denyer, M. C. T., & Youseffi, M. (2011). Imaging via widefield surface plasmon resonance microscope for studying bone cell interactions with micropatterned ECM proteins. Journal of microscopy, 241(3), 282-290.

Shen, K., Qi, J., & Kam, L. C. (2008). Microcontact printing of proteins for cell biology. JoVE (Journal of Visualized Experiments), (22), e1065-e1065.

Su, W. T., Liao, Y. F., & Chu, I. M. (2007). Observation of fibroblast motility on a micro-grooved hydrophobic elastomer substrate with different geometric characteristics. Micron, 38(3), 278-285.

Tan, J. L., Liu, W., Nelson, C. M., Raghavan, S., & Chen, C. S. (2004). Simple approach to micropattern cells on common culture substrates by tuning substrate wettability. Tissue engineering, 10(5-6), 865-872.

Whitesides, G. M. (2006). The origins and the future of microfluidics. Nature, 442(7101), 368-373.

Yea, K. H., Lee, S., Choo, J., Oh, C. H., & Lee, S. (2006). Fast and sensitive analysis of DNA hybridization in a PDMS micro-fluidic channel using fluorescence resonance energy transfer. Chemical Communications, (14), 1509-1511.

Zhang, X., Kang, L. G., Ding, L., Vranic, S., Gatalica, Z., & Wang, Z. Y. (2011). A positive feedback loop of ER-α36/EGFR promotes malignant growth of ER-negative breast cancer cells. Oncogene, 30(7), pp. 770-780.

Zhu, B., Lu, Q., Yin, J., Hu, J., & Wang, Z. (2005). Alignment of osteoblast-like cells and cell-produced collagen matrix induced by nanogrooves. Tissue engineering, 11(5-6), 825-834.

*Journal of Science and Technology in the Tropics* (2017) 13(1): 75-84

# Gamma-domain Brainwave Stimulation using Isochronic Tones

**Deraman, S.N. and [1]David, N.V.**
Faculty of Mechanical Engineering, Universiti Teknologi MARA, 40450 Shah Alam, Selangor, Malaysia
[*]Correspondence author email: davidfkm@salam.uitm.edu.my

Received: 02 July 2017; Accepted: 30 Sept 2017

**Abstract** The surge of electric pulses and chemical reactions in human brain produce brain waves at five distinct frequency domains between 0.5 Hz and 100 Hz. These domains are associated with different brain activities and characterize different mental states. The cerebral brain cells, which produce the frequency patterns in accordance to the brain activity, can be synchronized to or resonated at a desired frequency by externally stimulating the cells using acoustical means including binaural beats (BB) and isochronic tones (IT). IT are single frequency tones that can be easily generated and perceived by the brain whereas BB are auditory brainstem responses originating from the decomposition of two tones. The states of alertness and focus can be traced to areas within the frontal lobes of the brain at gamma range of brainwave frequencies, i. e. circa 40 Hz and above. This paper presents the preliminary investigation on the effectiveness of IT over BB on stimulating the mental states of alertness and attention on human brain at the gamma domain. A maiden group of ten healthy male human subjects are chosen for this purpose. Electroencephalograph signals of the evoked potential due to resonance of the prefrontal cortex (PFC) with the induced aural stimuli are measured. It is observed that the root-mean-square values of the potentials recorded at the anterior front electrode locations namely, AF3 and AF4, after exposition to IT increased by an average of 15% over that measured post exposition to BB. Similar observation is made at the frontal right (F4) location, which has a greater influence of the mental states mentioned above. The results indicate that IT has an improved effect than BB on the potentials measured at the PFC locations and render a positive influence on the focus and attention mental states of the brain.

**Keywords**-brainwave stimulation; binaural beats; isochronic tones; gamma brainwave; bio-potential

## INTRODUCTION

The surge of electric pulses and chemical reactions in human brain produce brain waves at frequencies between 0.5 Hz and 100 Hz. Brainwave entrainment is a phenomenon of changing brain waves from one frequency to another frequency. It is a process that typically uses an audio and/or visual stimulation to alter brain wave patterns and thereby to recreate certain states of minds [1]. Different areas of the brain emanate waves at different frequencies. These areas reverberate or beat at their respective frequencies when stimulated by external audio signals that are identical or near to those frequencies [2]. This phenomenon

is called as Frequency Follow Response or simply known as entrainment [3]. In brainwave entrainment, the brain will be entrained or synchronized to a precisely applied audio frequency that will be followed by certain areas of the brain.

There are five brainwave frequency domains that include gamma, beta, alpha, theta and delta. Each domain corresponds to unique brain functions or mental states as shown in Fig. 1. Recent studies indicate that pain states like anxiety and stress can be lightened by brainwave entrainment [1,4,5]. Mental states such as sleep, relaxation, consciousness, attention and alertness could also be enhanced via synchronization of brainwave to the respective frequency domains [6,7].

Of all the five frequency ranges shown in Fig. 1, the gamma and beta domains are more related to mental states such as concentration, attention, judgment and problem solving [8,9,10]. The gamma domain, which ranges between about 30 Hz to 100 Hz, corresponds to attention and focus. These physiological functions are mostly performed in the prefrontal cortex areas of the brain as shown in Fig 2. However, the gamma frequency domain is not completely independent from other sub-domains arising from attention related daily activities that the brain is subject to [9]. Stimulation of frequencies nearer to the lower cut-off of the gamma range is expected to assist in enhancing the attention and alertness mental states.

Binaural beats (BB) are auditory brainstem responses in each hemisphere of the brain. They can be generated by simultaneously applying two tones at slightly different frequencies to the left and right ears, respectively. The resulting discrepancy between the two tones is perceived as BB by the brain [14,15]. For example, when a pure tone of 500 Hz is provided to the right ear and a pure tone of 510 Hz is supplied to the left ear, the brain identifies the difference of 10 Hz as auditory beats [16,17]. Two tones with a frequency difference of as low as 0.5 Hz can be recognized by the brain as BB. The human ear can only detect sound ranging from 20 to 20,000 Hz with decreasing sensitivity at both ends of the spectrum [11]. Brainwave frequencies, as illustrated in Fig. 1, lie in the range of 100 Hz and below. BB, which are generated at frequencies below the audible range, are thus advantageous to the process of brainwave synchronization over direct application of sound signals at subsonic frequencies.

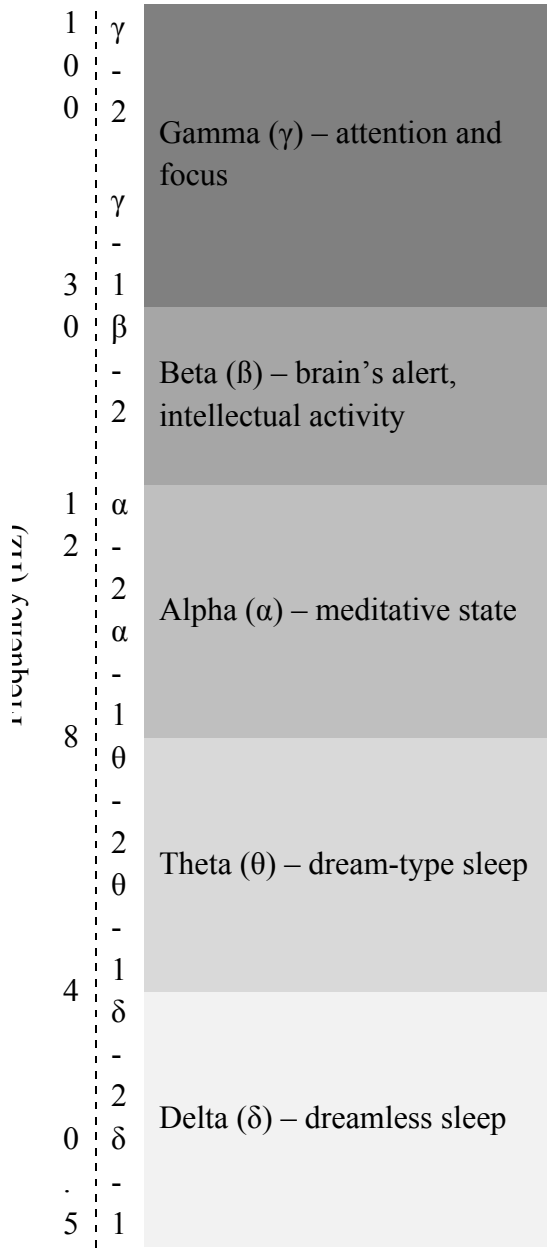


Fig. 1. Brain waves patterns and the corresponding frequency bands (designed after [8,11–13]).

Isochronic tones (IT) are single frequency tones that can be easily generated and perceived by the brain. Isochronic tones can be described as quick pulses of single tone sound. The brain is entrained to the frequency of the pulses. Isochronic tones, which are single tone audio signals, have been found to entail a strong auditory evoked response by the brain compared to BB [18]. Therefore, IT is expected to be perceived more effectively by the brain compared to BB. It also can be played through regular speakers and does not require headphones. However, IT is inapt for brainwave entrainment below 4 Hz [19].

Brain waves can be detected and recorded using methods such as electroencephalography (EEG), magneto encephalography (MEG) or magnetic resonance imaging (MRI). Electroencephalograph signals of the evoked potential of the brain due to external stimuli are easier to be recorded and simpler to be analyzed using the EEG method compared to the other

two methods [11]. This paper presents the preliminary investigation on the effectiveness of IT over BB on stimulating the mental states of alertness and attention on human brain at the gamma domain.

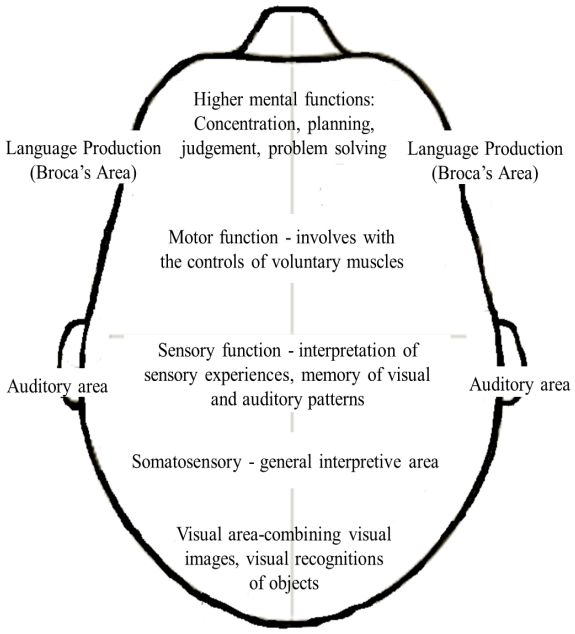


Fig. 2. Physiological function of the brain (designed after [8–10]).

## METHODOLOGY

### *A. Participant selection and ethical consent*

The test participants (i.e., human subjects) for the purpose of this study were gathered via an advertisement opened to all staff and students at Universiti Teknologi MARA (UiTM). 10 male subjects between 18 and 30 years old participated in the test. The subjects are all in best of health condition, have normal hearing and vision, and are free from any reported history of neurological or psychological illness. Written informed consent was obtained from each subject before their participation in the test. All participants were given remuneration for their involvement. Female subjects were not included in this study due to uncertain emotional and empathy mental states during their menstrual cycle [20]–[22]. This study is approved by UiTM Research Ethics Committee.

### *B. Equipment*

Two types of audio signals are employed for this experimental study. The BB and IT used in this study were extracted from mindamend.com (free videos). The signals comprise of 40 Hz BB and 40 Hz IT. Emotiv EPOC$^{TM}$ is used to record the EEG signals. The felt-based sensors of the headset electrodes in this wireless EEG system are moistened with a saline liquid to reduce contact impedance.

The placement of the electrodes follows the International 10/20 System of Electrode Placement. The electrode placements on the scalp are labeled AF3, AF4, F3, F4, F7, F8, FC5, FC6, P3 (reference 1, CMS), P4 (reference 2, DRL), P7, P8, T7, T8, O1 and O2, as

indicated in Fig. 3. The bio-potential signals acquired from all channels are compared with the CMS reference level for noise reduction. Data obtained from four channels, namely the AF3, AF4, F3 and F4, are used in the analysis for the purpose of this study. These channels are chosen due to their locations that correspond to the attention and focus functions of the brain as depicted in Fig. 2.

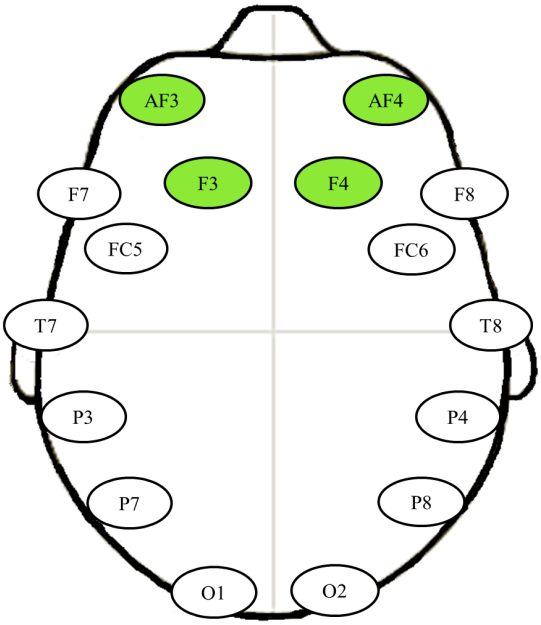


Fig. 3. Electrodes locations as per the International 10/20 System of Electrode Placement.

*Procedure*

Each participant took part in two sets of experiments, i.e. one each for BB and IT. As illustrated in Fig. 4, the test procedure and thereby the total test period of 22 minutes is divided into three main stages. The first stage pertains to a two-minute baseline EEG recording of the subjects in a relaxed mental condition. Prior to this stage, the subjects were suggested to drink water and were requested to sit comfortably and relax while their eyes closed in an illuminated ambient. The subjects are encouraged to restrict bodily movements especially of the head (including eye blink) that could interfere with the EEG recording. The subjects are thereby conditioned to a calm state to prepare them for the synchronization stage.

The second stage involves 15 minutes exposure of the subjects to BB or IT. The EEG signals are recorded during the last two minutes of the second stage and the root-mean-square (RMS) values of the evoked potentials, which also indicate the power content of the signals, are determined for the purpose of this study.

Subsequent to this, the audio signals are turned off and the subjects are requested to continue to sit while their EEG potentials are recorded for five minutes. This third stage post to the exposition of BB or IT pertains to the measurement of the evoked potentials under synchronized mental state for the given period of time. The analysis of the post-exposition results and the full effect of synchronization will be treated as a separate subject of study in another paper.

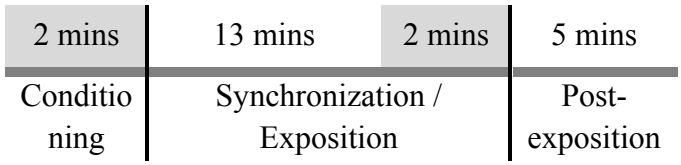


Fig. 4. Experimental procedure (shaded region correspond to EEG recording period and analysis for the purpose of this study)

## RESULTS AND DISCUSSION

Fig. 5 shows the baseline RMS values of the EEG potentials measured at the four selected channels namely, AF3, AF4, F3 and F4, during the conditioning stage. All the potential values are found to be lesser than that measured after the exposition to BB and IT, as will be discussed next.

Figs. 6 and 7 show the evoked potential responses measured at the four electrode locations in the anterior frontal (AF) and frontal (F) areas as indicated in Fig. 3, respectively. It is observed that the highest RMS value of the potentials measured in the AF area as shown in Fig. 6 is 33.40 μV for AF4-IT and the lowest value is 27.19 μV for AF4-BB. The potentials recorded for AF3-IT and AF3-BB are 30.96 μV and 28.69 μV, respectively.

Fig. 7 shows the RMS values of the potentials obtained at the F3 and F4 areas. The greatest potential value measured is for F4-IT (26.80 μV) and the lowest is for F3-IT (22.15 μV). The latter is about the value recorded for F3-BB (23.87 μV), i.e. with a ~ 7.8% difference.

It can be determined from Fig. 6 that the potentials measured for IT is greater than for BB by 7.9% and 22.8% for the AF3 and AF4 locations, respectively. Similarly, the F4 channel in the frontal region also registered 16.2% greater potential value for IT compared to BB (see Fig. 7). Clearly, IT has a stronger influence on the brainwave synchronization than BB and hence the higher evoked potential of the subjects at the selected electrode locations.

Fig. 2 above shows that the AF3, AF4, F3 and F4 locations are areas related to mental states such as concentration, alertness and judgment. The potential values measured for IT at the AF3 (30.96 μV) and AF4 (33.40 μV) channels are greater compared to that registered at F3 (22.15 μV) and F4 (26.80 μV). This illustrates the better response of the anterior frontal area to the applied gamma IT.

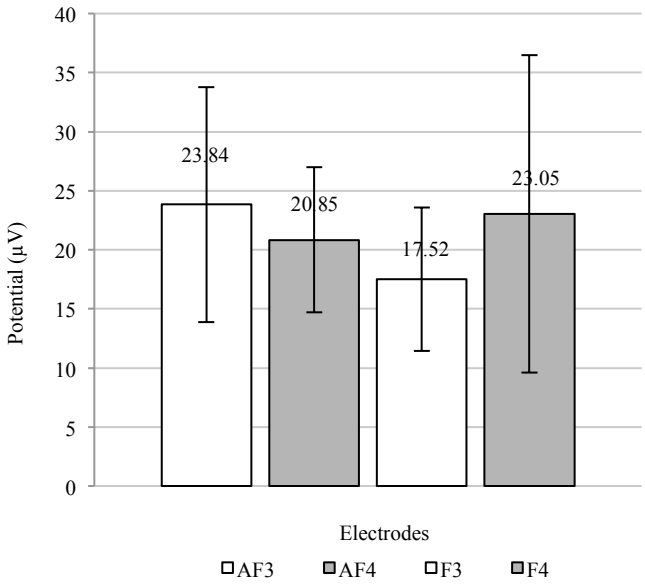


Fig. 5. Baseline measurement of EEG potential during the conditioning stage.

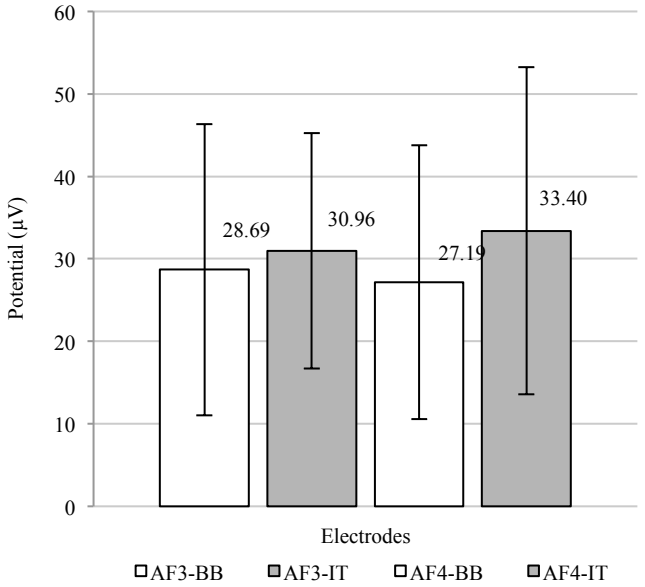


Fig. 6. EEG signals measured at AF3 and AF4 electrode locations for BB and IT.

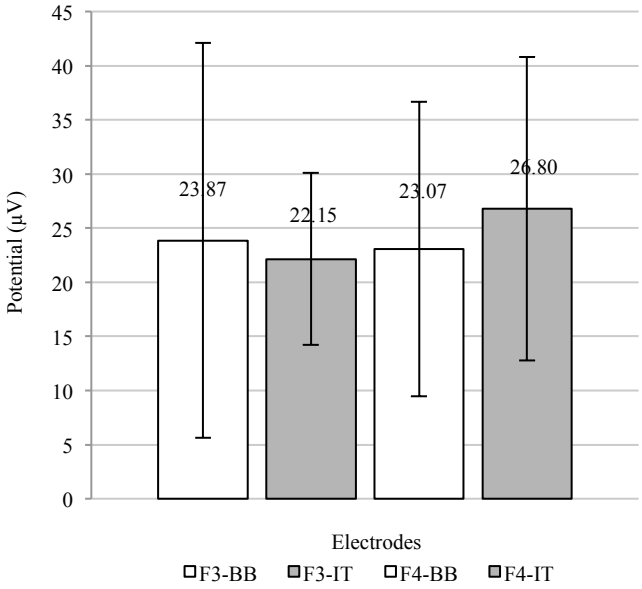


Fig. 7. EEG signals measured at F3 and F4 electrode locations for BB and IT.

Both the AF4 and F4 channels in the right hemisphere of the brain recorded higher evoked potentials that than their left counterpart to the applied gamma IT. The potentials measured at the AF4 and F4 channels are greater than that of the baseline values (see Fig. 5) by 60.2% and 16.2%, respectively. Similar trend is observed for the BB but the increase is only by 30.4% and 0.1% for, in order, the AF4 and F4 channels.

It is clear from the discussion above that those channels responded well to the applied gamma frequency especially for IT. This reflects the effectiveness of the IT at a gamma rhythm of 40 Hz to alter the brainwave pattern into concentration or attention condition.

## CONCLUSION

The root-mean-square values of the evoked potentials recorded at the anterior front electrode locations namely, AF3 and AF4, upon exposition to IT increased by an average of 15% over that measured post exposition to BB. Similar observation is made at the frontal right (F4) location, which has a greater influence of the mental states mentioned above. The bio-signal data obtained in this study indicate that IT has an improved effect than BB on the potentials measured at the PFC locations and shall render a positive influence on the focus and attention mental states of the brain. However, exposure to pure tones or beats alone can be annoying and stressful to the listener. Further studies are essential to verify if tones and beats embedded in a pleasant background audio will be as effective but less bothersome to the subject and a more exhilarating way of brainwave entrainment.

### ACKNOWLEDGMENT

The work reported here is funded by the Ministry of Education Malaysia under the auspices of the Exploratory Research Grant Scheme (ERGS). This support is gratefully acknowledged.

The Research Management Institute of Universiti Teknologi MARA (UiTM) is thanked for its grant management and administration services.

## REFERENCES

[1] T. L. Huang, C. Charyton, "A comprehensive review of the psychological effects of brainwave entrainment," Altern. Ther. Health Med., vol. 14, pp. 38-50, Sept 2008.

[2] U. Will, E. Berg, "Brain wave synchronization and entrainment to periodic acoustic stimuli," Neurosci. Lett., vol. 424, pp. 55-60, Jul 2007.

[3] J. C. Smith, J. T. Marsh, W. S. Brown, "Far-field recorded frequency-following responses: Evidence for the locus of brainstem sources," Electroencephalogr. Clin. Neurophysiol., vol. 39, pp. 465-472, Nov 1975.

[4] R. Padmanabhan, A. J. Hildreth, D. Laws, "A prospective, randomised, controlled study examining binaural beat audio and pre-operative anxiety in patients undergoing general anaesthesia for day case surgery," Anaesthesia, vol. 60, pp. 874-877, Apr 2005.

[5] Y. Mu, Y. Fan, L. Mao, S. Han, "Event-related theta and alpha oscillations mediate empathy for pain," Brain Res., vol. 1234, pp. 128-136, Jul 2008.

[6] F. H. Atwater, "Accessing anomalous states of consciousness with a binaural beat technology," J. Sci. Explor., vol. 11, pp. 263-274, 1997.

[7] A.Zauner, R. Fellinger, J. Gross, S. Hanslmayr, K. Shapiro, W.Gruber, S. Müller, W. Klimesch, "Alpha entrainment is responsible for the attentional blink phenomenon," NeuroImage, vol. 63, pp. 674-686, June 2012.

[8] M. van Wingerden, V. Martin, J.V. Lankelma, and C.M.A. Pennartz, "Learning-associated gamma-band phase-locking of action–outcome selective neurons in orbitofrontal cortex," J. Neurosci., pp. 10025-10038, Jul 2010.

[9] N. Kopell, G. B. Ermentrout, M. A. Whittington, R. D. Traub, "Gamma rhythms and beta rhythms have different synchronization properties," PNAS, vol. 97, pp. 1867–1872, Feb 2000.

[10] M. Ainsworth, S. Lee, M. O. Cunningham, A. K. Roopun, R. D. Traub, N. J. Kopell, M. A. Whittington, "Dual gamma rhythm generators control interlaminar synchrony in auditory cortex", J. Neurosci., pp. 17040–17051, Nov 2011.

[11] M. F. Bear, B. W. Connors, M. A. Paradiso, "Brain rhythms and sleep," Neuroscience exploring the brain, 3rd ed. Baltimore, Lippincott Williams & Wilkins, ch. 19, pp. 586-592, 2001.

[12] M. Teplan, A. Krakovska, "EEG features of psycho-physiological relaxation," Proc 2nd Int. Symp. Appl. Sci. Biomed. Commun. Tech. 2009, pp. 1-4, 2009.

[13] R.C. Filimon, "Beneficial subliminal music: binaural beats, hemi-sync and metamusic," Proc 11th WSEAS Int. Conf. Acoust. and Music: Theory and Appl., pp. 103-108, 2010.

[14] G. Oster, "Auditory beats in the brain," Sci. Am., pp. 94-102, 1973.

[15] H. Wahbeh, C. Calabrese, H. Zwickey, "Binaural beat technology in humans: a pilot study to assess psychologic and physiologic effects," J. Altern. Complement. Med., vol. 13, pp. 25-32, Mar 2007.

[16] J. D. Lane, S. J. Kasian, J. E. Owens, G. R. Marsh, "Binaural auditory beats affect vigilance performance and mood," Physiol. & Behavior, vol. 63, pp. 249–252, Aug 1998.

[17] J. H. Grose, E. Buss, J. W. Hall III, "Binaural beat salience," Hearing Res., vol. 285, pp. 40-45, Jan 2012.

[18] D. Siever, "Audio-visual entrainment: 1. History and physiological mechanisms," Biofeedback, vol. 31, pp. 21-27, Aug 2006.

[19] H. A., Westfall, "The effect of visual search and audio-visual entrainment on episodic memory," Dissertation – Graduate School Theses and Dissertations, Univ. of South Florida, pp. 23-26, Jan 2013.

[20] W. Zhang, R. Zhou, Q. Wang, Y. Zhao, Y. Liu, "Sensitivity of the late positive potentials evoked by emotional pictures to neuroticism during the menstrual cycle," Neurosci. Lett., vol. 553, pp. 7-12, June 2013.

[21] N. K. Ferree, R. Kamat, L. Cahill, "Influences of menstrual cycle position and sex hormone levels on spontaneous intrusive recollections following emotional stimuli," Conscious. Cogn., vol. 20, pp. 1154-1162, Dec 2011.

[22] B. Derntla, R. L. Hack, I. Kryspin-Exner, U. Habel, "Association of menstrual cycle phase with the core components of empathy," Horm. Behav., vol. 63, pp. 97-104, Jan 2013.

*Journal of Science and Technology in the Tropics* (2017) 13(2): 85 - 102

# Root System withholding Strength for River Bank

**Ding Ibau and Ruslan Hassan**
Malaysia Institute of Transport (Mitrans) UiTM, 40450 Shah Alam, Selangor
[*]**Corresponding author email:** drruslan@yahoo.com

Received: 20 Aug 2017; Accepted: 30 Oct 2017

**ABSTRACT** The ability of vegetation to stabilise soils is frequently employed in slope stabilisation projects including riverbank restoration activity. Soil block samples permeated with roots of *Bermuda Grass* commonly used for remediation and riverbank restoration were tested in a direct shear apparatus. Shear stress results of rooted soils were compared with results of un-vegetated soil blocks with similar soil types. The increase of shear strength was determined by comparing shear stresses at specific horizontal displacements. The relative strength increase at the same displacement was 27.3 kPa compared to 19.1 kPa for un-vegetated soil at a displacement of 13.3cm (Location 3). The relative strength increase at the same displacement of 13.3 cm was 43.5 % for Location 1 and 42.4 % for Location 2. The shear stresses in most of the blocks with roots were still increasing at the end of the test (maximum displacement of about 15 cm). These conservative root biomass values and the shearing resistance obtained can be used in the assessment of the stability of the existing vegetated slopes and in the design of vegetated riverbanks.

## INTRODUCTION

The physical vegetative coverage on stream-banks provides underground soil reinforcement and surface protection from scour. The level of vegetation for protecting soil depends on the combined effects of roots, stems and foliage. Root systems aid stream-bank stabilisation through soil-root interaction. The mechanics of root-reinforcements are similar to the basic mechanics of engineered reinforced-earth systems. Vegetation installed on slopes and stream-banks provides resistance to shallow mass movement by counterbalancing local instabilities.

## STABILISING MECHANISMS

For stabilisation techniques that rely on vegetative materials, the stabilisation is vulnerable at the early stage but becomes stronger as the vegetation is established. The primary stabilising mechanisms include :

(a) Reinforcing the soil with tensile fibres of the root mass,

(b) Increasing shear strength by reducing pore-pressures through transpiration,

(c) Anchoring the slope through deep root penetration into more stable strata, and

(d) Decreasing the flow velocities and dissipating the flow energies by redistributing the flow pattern and direction by the foliage and stems of shrubs.

Perhaps the most complete overview of soil reinforcement by roots and artificial fibres is provided by Gray and Sotir [1] The basic process involves the transfer of shear stress within the soil to tensile resistance of the roots, which becomes a function of the interface friction along the root surface. The orientation of the fibre relative to the shear force, the skin friction of the root, the elongation behaviour of the root, the fraction of the soil cross section occupied by roots, and the tendency to break rather than pull out are all factors influencing the reinforcing effect. Over the last 60 years, data related to limits of vegetal reinforcement have been presented both in terms of shear stress (or tractive force) and flow velocities. Shear stress, in $N/m^2$, is a preferred measure because it considers several variables including depth, the wetted channel perimeter, and flow velocities. In addition, failure criteria for a particular lining is represented by a single shear stress value, applicable over a wide range of channel slopes and shapes. For these reasons, this paper will present vegetal resistance in terms of shear stress.

## THEORETICAL CONSIDERATION

Soil is strong in compression but weak in tension and roots are weak in compression but strong in tension. Therefore when soil and roots are combined the resultant soil-root matrix produces a mass which is much stronger than either the soil or the roots on their own. The roots act by transferring the shear stresses developing in the soil to the tensile resistance in the roots, and also by distributing stresses through the soil, so avoiding local stress build-ups and progressive failures. These will be highly dependent on the contribution of root density.

The theory of reinforced earth was first developed by Vidal [2]. As a vertical principal stress is applied to an unconfined element of soil the element will strain laterally as it compresses axially (Figure 1). If reinforcement is added to the soil in the form of horizontal strips, the lateral movement induced in the soil generates a frictional force between the soil and the reinforcement. As a tensile force develops within the reinforcement a corresponding compressive lateral confining stress is generated within the soil. This lateral confining stress is analogous to an externally applied confining pressure and is proportional to the applied normal confining stress up to a limit defined as the ‘critical confining stress’. The action of reinforcement in soil is therefore not one of carrying developed tensile stresses but of the anisotropic reduction or suppression of an applied normal strain rate. This suppressive mechanism leads to the concept of anisotropic cohesion.

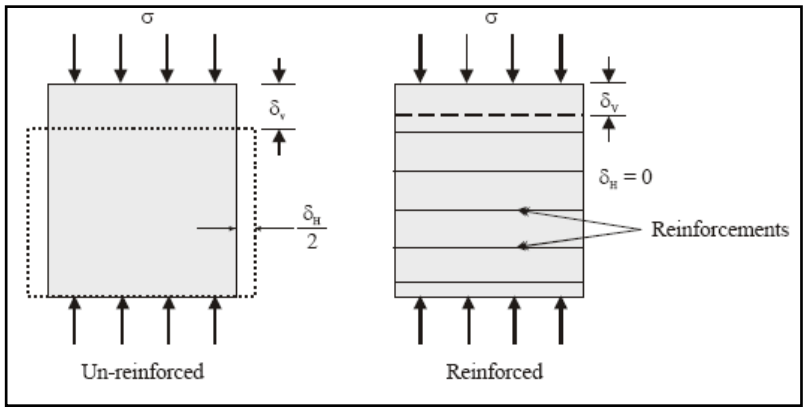


**Figure 1: The action of reinforcements on a cohesionless soil element**

Note: The reinforced element resists lateral expansion through the mobilization of a frictional force between the soil and the reinforcement [3]

Some studies indicate that the increase in apparent soil cohesion is limited to roots up to about 2 cm in diameter [4]. Beyond this size the reinforcing effect is thought to be largely due to a root's ability to anchor a relatively weak layer of soil across a discontinuity, the shear surface, to an underlying stronger soil or bedrock. The justification for this limit is not completely clear as field studies often cited as supporting it [5, 6], although demonstrating the importance of small roots to increased soil shear strength does not actually measure the effect of larger roots. Burroughs & Thomas [5] measured roots up to 1 cm in diameter, and O'Loughlin & Watson [6] up to 3 cm. An extensive literature search was unable to locate any study that assessed the reinforcing actions of roots of different sizes. There are also many examples of small roots (< 2 cm diameter) acting or suspected as acting like ground anchors by growing into discontinuities and fissures in the bedrock or more stable substrate [7, 8]. It is generally agreed that apart from an increase in apparent soil cohesion roots may also increase the shear strength of a soil by an anchoring mechanism.

**A. Root system**

Investigations of root system architecture include those undertaken on vegetative crops for growth analysis [9, 10], mathematical models of root structure form and geometry [11, 12, 13, 14, 15], and general rooting habits as they relate to site conditions and processes [16, 17. 18]. Evidently there is an extremely wide range in root geometry from species to species (Figure 2) and so it is difficult to transfer data directly from one site to another because of the influence of local site conditions on root growth [19]. Different rooting habit and site condition will influence the root biomass density. This theory also agreed by Todd, *et.al* [20]; for different species of vegetation will give different root geometry and this will give different values of density. The plant species, root density, and stem height were inconsistent because of variation on soil types.

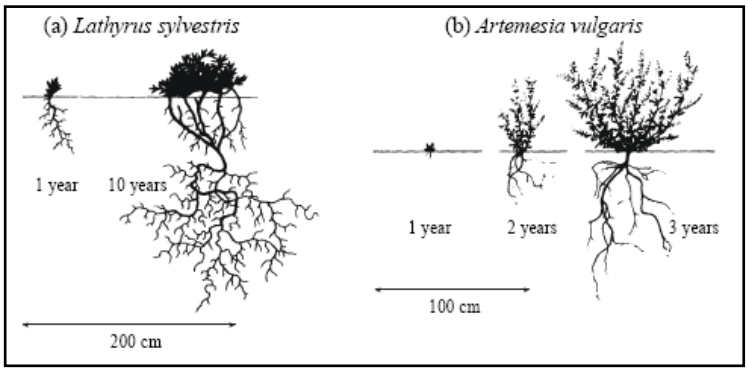


**Figure 2: Some examples of the wide variety in root geometry of different species. (a) *Lathyrus sylvestris* and (b) *Artemesia vulgaris* (after Schiechtl [21])**

**B. Soil mass shear strength**

The strength of soil is difficult to be measured directly. Evaluating the effect of roots on soil strength increases that difficulty. In 1968 a shear box was developed to measure the contribution of small alder *(Alnus glutinosa)* roots to the strength of relatively homogeneous nursery soil in Japan. The weight of roots attained 53% of the variation in measured soil strength. The shear box was later modified to study the contribution to soil strength by roots of a mixed old-growth forest of Douglas-fir *(Pseudotsu-gamenziesii),* western redcedar *(Thuja plicata),* and western hemlock *(Tsuga heterophylla)* growing on glacial till sub-soils in British Columbia, Canada. The weight of roots in the soil sample was the most significant of seven variables tested, accounting for 56% of the variation in measured soil strength. Shear box was used in the testing of relatively simple soil-root system of a mature shore pine *(Pinus contorta)* forest growing on coastal sands in northern California. The dry weight of the live roots less than 17 mm in diameter was the significant variable contributing to soil shear strength among the soil and vegetative variables tested. The shear box tests resulted in Eq. (1), in which soil strength is in kilopascals and root biomass is in kilograms per cubic meter.

$$\text{Soil strength} = 3.13 + 3.31 \text{ root biomass} \quad (1)$$

The equation attains 79% of the variation in measured soil strength. The mean biomass of the less than 17-mm-diameter live roots was 1.77 kg/m$^3$, which represented 64% of the total root biomass. To evaluate the contribution of root in the strength of soil-plant mass, dry density biomass of vegetative is a dominant component in relation to the soil strength.

**C. Significant roles of roots system and configuration**

Roots system plays significant role in plant-soil mass in order to improve slope and prevent soil erosion. There has been a long held belief that erosion control performance by vegetation

relates to the additional strength provided by vegetation roots to the soil as well as the ability of the above-ground parts to intercept and transpire water. The role played by vegetation in improving slope stability and preventing soil erosion is well recognized [22, 23, 24].

In order to evaluate the contribution of vegetation roots to soil shear strength (i.e. to determine $S_r$) a simple model was developed independently by Waldron (25) and Wu *et al*. [26]. The model was designed to simulate the idealised situation of vegetation's vertical roots extending across a potential sliding surface in a slope. It consists of a flexible, elastic root extending vertically across a horizontal shear zone of thickness z (Figure 3).

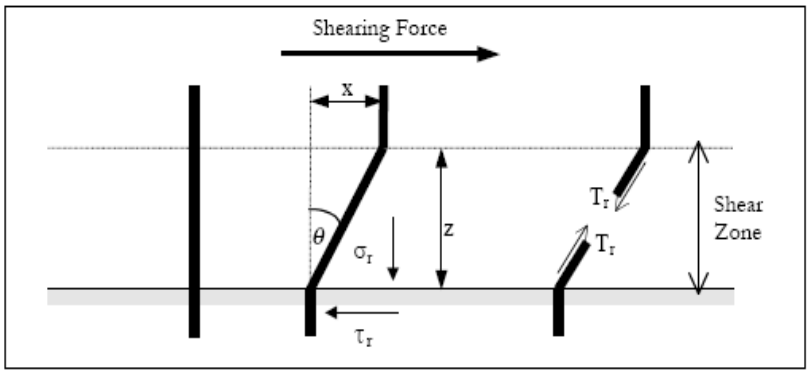


**Figure 3: Model of a flexible, elastic root extending vertically across a horizontal shear zone.**

As the soil is sheared a tensile force $T_r$ develops in the roots. As shown in Figure 3 this force is resolved into a tangential component (tr) which resists shear and a normal component (sr) which increases the confining stress on the shear plane

$$\tau_x = \tau_s \sin\theta \text{ and } \sigma_x = \tau_s \cos\theta \quad (2)$$

where **(tr)** and (sr) are the tangential and normal stresses applied to the soil by $T_r$; ($t_s$) is the average tensile strength of roots per unit area of soil; and $\theta$ is the angle of shear distortion of the root.

The contribution of the root to shear strength is then given by:

$$S_r = \sigma_x \tan\phi + \tau_x = \tau_s(\cos\theta \tan\phi + \sin\theta) \quad (3)$$

where $\phi$ = angle of internal friction.

The average tensile strength of the roots per unit area of soil ($t_s$) is determined by multiplying the average tensile strength of the roots by the fraction of the shear surface cross section occupied by roots:

$$\tau_s = T_s (A_s/A) \quad (4)$$

## METHODOLOGY

The study involved both field and laboratory studies. Soil blocks were obtained from a site at Jenderam Hulu River in Sepang. The samples were taken from 4 locations at the site and all the testing and analysis were carried out in the Water Laboratory and Advanced Soil Laboratory. The soil blocks from the riverbank were considered very suitable for this study because the plants (Bermuda grass (*cynodon dactylon*) were all growing in close proximity and access was possible. The location for each of the samples is shown Figure 4.


**Figure 4. Sampling Locations**

### A. Materials and Methods

Four sample blocks of soil (each location) were removed from a riparian environment with caution to minimize disturbance of soil structure. All samples were carefully carved to dimensions of 100 mm by 100 mm by 30 mm depth. Samples from the bare location contained no vegetation, but serve as a typical soil. Samples from location 1, 2 and 3 (Figure 4) contained the single specimen of vegetative, estimated at 2.5 years in age, with roots radiating throughout the soil block.

**Figure 5: Samples of vegetated location (w/out vegetation), 1, 2 and 3)**

When samples were collected and tested, the soil moisture levels were at the field capacity. The shear box machine (ELE International) was used in this study. The block samples were taken using a sharp edged metal plate box with dimensions of 100 x 100 x 30 mm. All samples had been carefully carved and removed with caution to minimize disturbance. Three block samples were obtained for the 4 locations making a total of 12 block samples. The distances between samples were kept to a 1m radius and 10 m for each location containing vegetation to obtain blocks with similar soil types. Efforts were made to select uniform soil conditions, although the plants tended to be distributed according to variations in soil and hydrology (moisture content).

**B. Shear Test Description**

A direct shear apparatus shown in Figure 6 was modified to perform shear tests on the soil blocks. The dimensions of the shear box were selected to accommodate the soil blocks. Soil specimens were placed in the shear box machine. Where applicable, excess top growth was trimmed to facilitate handling and small gaps at the edges of the sample filled with identical soil using as low compaction effort. Load (stress) and displacement (strain) were plotted throughout the duration of the test procedure. A nominal normal load was applied in the form of a 2 kg metal plate to aid in the containment of the specimens during the test procedure; however, no other significant normal load was maintained in order to simulate natural surface soil conditions. The testing methodology followed ELE International procedure. All samples were tested with the matrix potential brought as close as possible to zero at the shear plane. A load cell was installed to measure the shear forces and an electronic device measured the horizontal displacements. Information from these two measuring devices was sent to the data logger (digital shear machine), which in turn fed the data into a computer. After the completion of the test, photographs of the sheared surface were taken, and the roots and top growth were removed to measure the dry biomass. The soil from each block (location of typical soil) was mixed and a sample taken for conducting a grain-size distribution analysis.

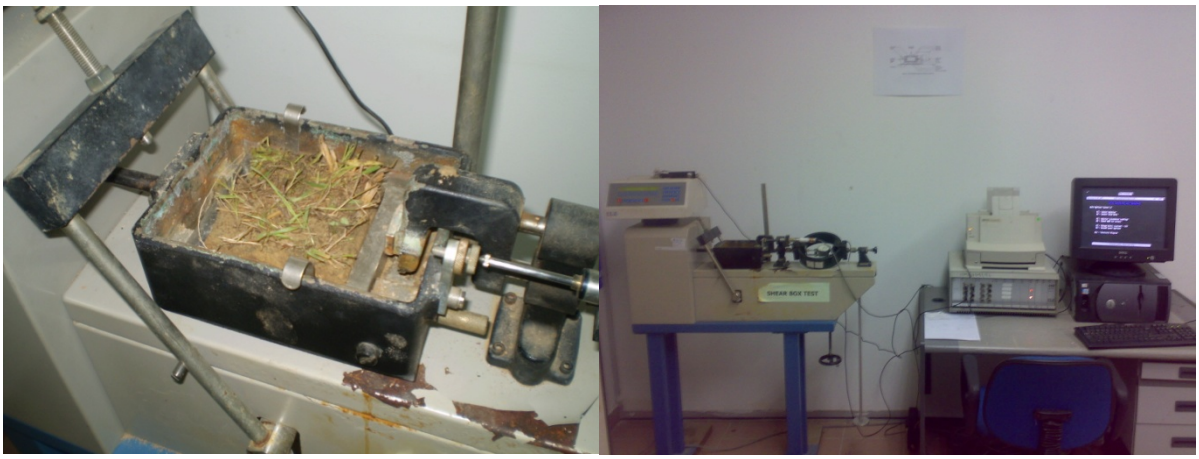

**Figure 6: Soil Block Placed in the Shear Box**

### C. Dry Biomass Test

Dry root biomass density is the dry weight of roots divided by the volume of the block sample used in the shear test. After the soil blocks were sieved, all roots were extracted, washed, and separated into live and dead fractions, dried at $70^0$C and weighed. From each test location, data were collected for soil and root variables. The results of the average root biomass density were then plotted.

## RESULTS

Shearing tests were performed on soil blocks that contained roots to study the contribution of roots to the shear strength in a case where the shear deformation is constrained to a thin zone. The shearing resistances of the soil-root system and the biomass of selected roots were measured. Additionally particle size and the moisture content plus the soil block were measured to determine the type and characteristics of soils. The roots were exposed after the test and their orientations and variation within the soil blocks were observed and used to explain the shear strength value. The root biomass and the shearing resistance of the soil-root system were estimated with known solutions and compared with all the theoretical data. None of the roots that passed through the shear zone failed in tension at the maximum displacement. As a consequence, the root resistance is much less than that found in a case where the failure surface is restricted to the boundary between a weak soil and a firm base and where roots are anchored in the firm base and fail in tension.

### A. Soil-plant shear strength

Shear stress vs. horizontal displacement curves are shown in Figures 7 to 10 for representative tests of each location and for the un-vegetated soil. The shear stresses in different root permeated soil samples changed in different ways as the soil block was displaced because of their different root orientations. Additionally, there were no major drop

in shear stress of most of the samples suggests that the roots had not failed in tension yet. The shear stresses in most block samples, were still increasing at the end of the tests. As a result, peak stresses and residual stresses were not clearly identified from these plots. The method adopted to assess the shear strength increase was to compare them at a specific horizontal displacement.

The maximum shear stress achieved in the un-vegetated soil was about 19.1 kPa, 18.1 kPa for sample 3 and both sample 1 & 2, respectively. A shear force versus horizontal displacement plot (Figure 7) for the un-vegetated soil blocks was used to determine the displacement at which the maximum shear force occurred. l. On average, the maximum force occurred at displacement 11.8 cm, 12.8 cm and 13.3 cm. Therefore, stresses at these displacements were used to characterize the soil shearing resistance. In addition, stresses at 4cm, 6cm 8cm and 10.8cm were also included for comparison. A graph of the average shear stresses at these three different displacements is presented in Figure 11. An analysis of data using statistic was conducted using the data of shear stress occurring at a displacement of 4 cm, 6 cm, 8 cm, 10.8 cm, 11.8 cm, 12.8 cm and 13.3 cm.

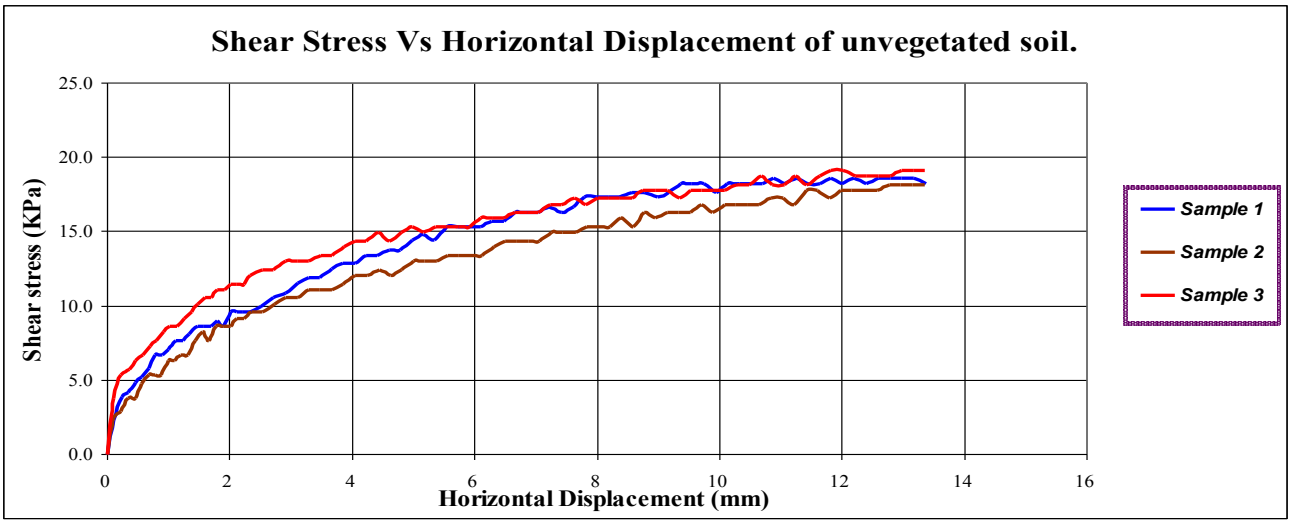


**Figure 7: Shear stress vs. horizontal displacement for representative samples of unvegetated soils.**

Sample one, un-vegetated soil, showed an ultimate shear stress of 19.1 KPa and a residual shear stress of 18.8 KPa. These values are typical of soils of similar particle size distribution at field capacity moisture levels. Visual inspection of the sample indicated that shear failure had occurred along a well-developed plane dissecting the entire soil block.

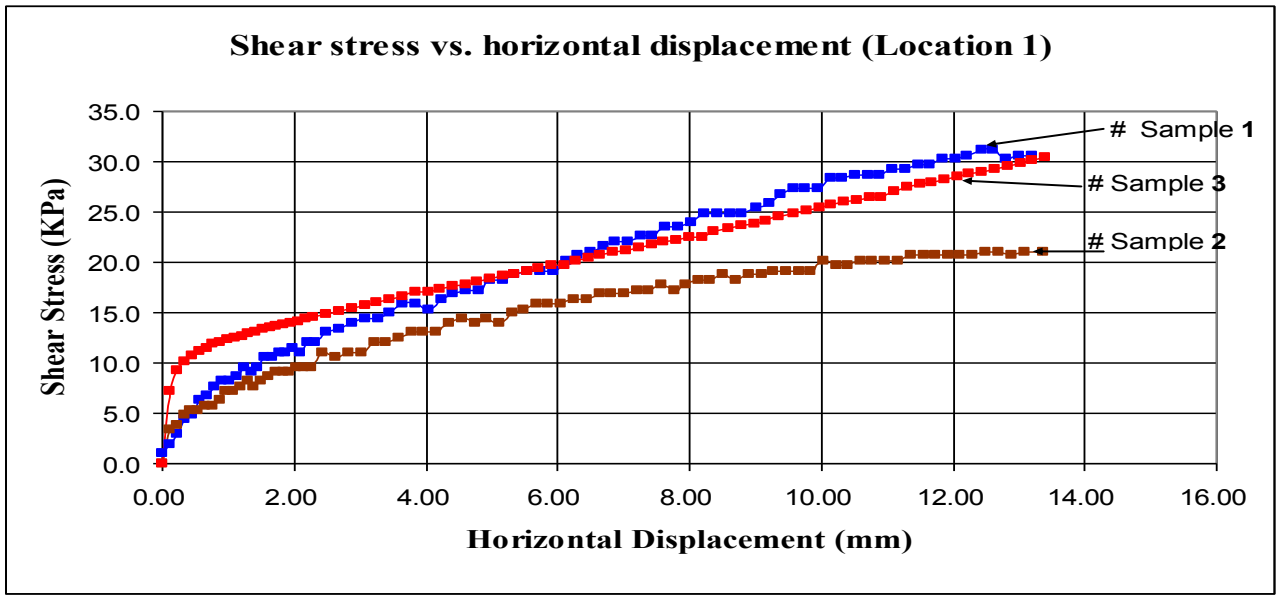


**Figure 8: Shear stress vs. horizontal displacement for representative samples**

Three samples, rooted with *Bermuda grass* at location 1, was tested until the full displacement capacity of the shear box machine had been utilized. The applied shear stress continued to climb steadily until a final reading of 30.6 KPa, 21.1 KPa and 30.6 KPa for samples 1,2 and 3 respectively (Figure 8) was taken before the test was terminated. Visual inspection of the sample indicated that shear deformation was distributed across a shear plan of soil reinforced by fibrous roots. This mode of shear deformation has been described by other investigator [26] as typical for soils with fibre inclusions. The magnitude of the shear resistance without discrete failure of soil structure was significantly higher than for un-vegetated soils, although the deformation mechanisms were the same. Reinforcement of soil by a substantially high density of fibrous roots, in this case, appeared to increase the strength of soils while also altering the failure mechanism. Interestingly, the plant and all its roots remained intact throughout the test procedure.

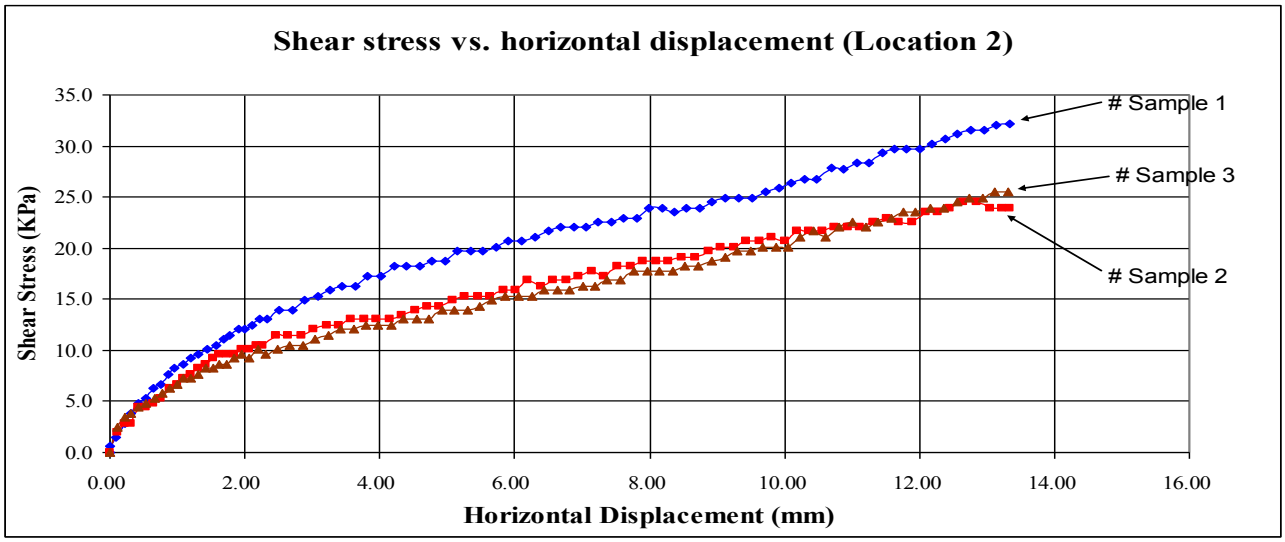

**Figure 9: Shear stress vs. horizontal displacement for representative samples**

Another 3 samples, rooted with the same grass at location 2, showed an ultimate shear stress of 32.2 KPa and a residual shear stress also 32.2 kPa (Figure 9 - sample 1). The observed failure mechanism was essentially identical to the un-vegetated soil, and noticeably slightly different from the samples at location 1, apparently due to the relatively low density (root biomass density) of fine fibrous roots as compared with the location 1 and 3. Both ultimate and residual shear stress values are higher than for un-vegetated soil, indicating the reinforcing value of the roots. Effects on the orientation, variation and morphology of the vegetation seem to give different value of shear resistance.

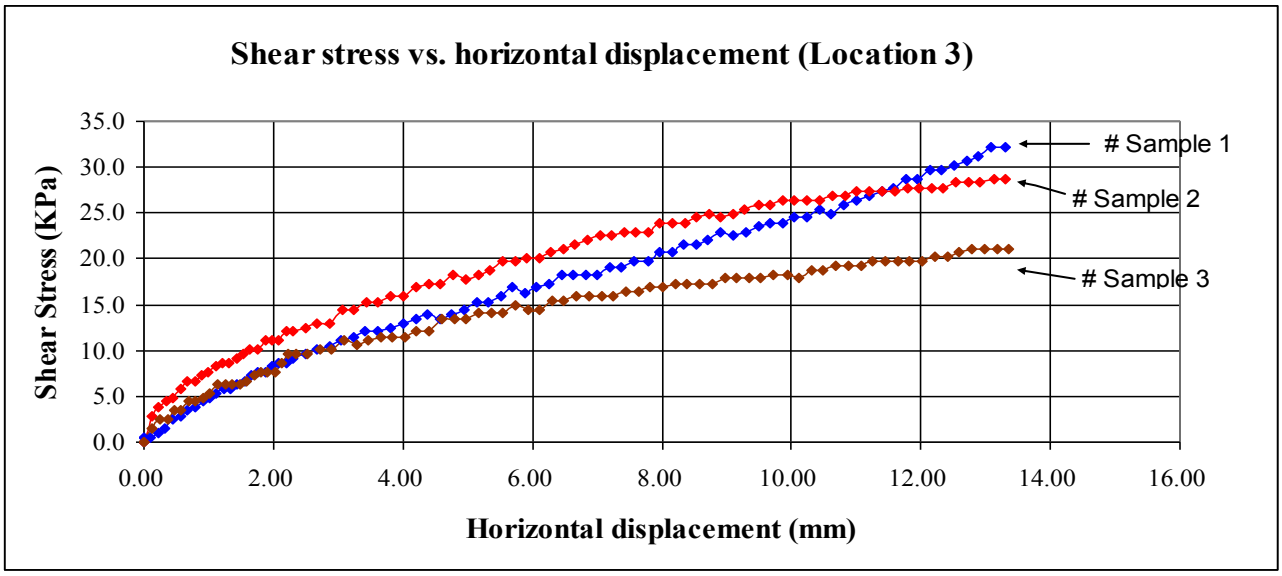


**Figure 10: Shear stress vs. horizontal displacement for representative samples**

The last three samples from location 3 also rooted with the same types of grass showed value of maximum shear stress of 32.2 kPa, 28.7 kPa and 21.1 kPa for sample 1, 2 and 3 respectively (see Figure 10). The magnitude of the shear stress of the soil-root matrix obtained at this location obviously higher than un-vegetated soils. The failure at the shear plan crossed by the roots was the same deformation mechanisms with the samples from other 2 locations. Reinforcement of soil by significant high density referring to the high root biomass density of fibrous roots, in this case, increases the strength of soils. (see Figure 12)

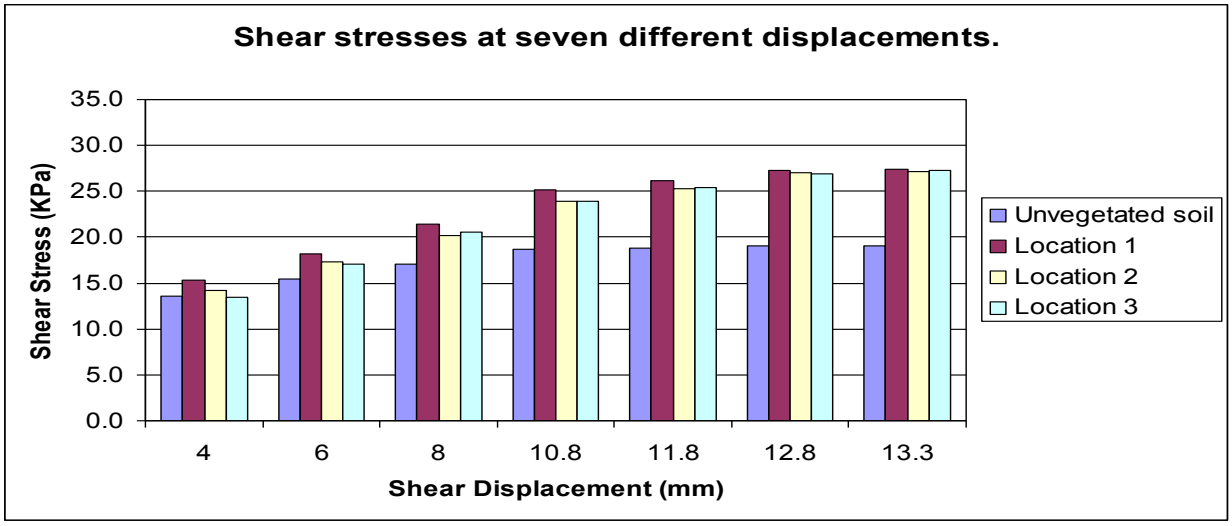


**Figure 11: Shear stresses at seven different displacements.**

## B. Root Biomass Density

The results of the average root biomass density are plotted in Figure 12. Dry root biomass density is the dry weight of roots divided by the volume of the block sample used in the shear test.

**Volume of soil Block:** 10cm x 10cm x 3cm = 300 $cm^3$
**Biomass** = (Weight of dry root)/ (Volume of soil block)

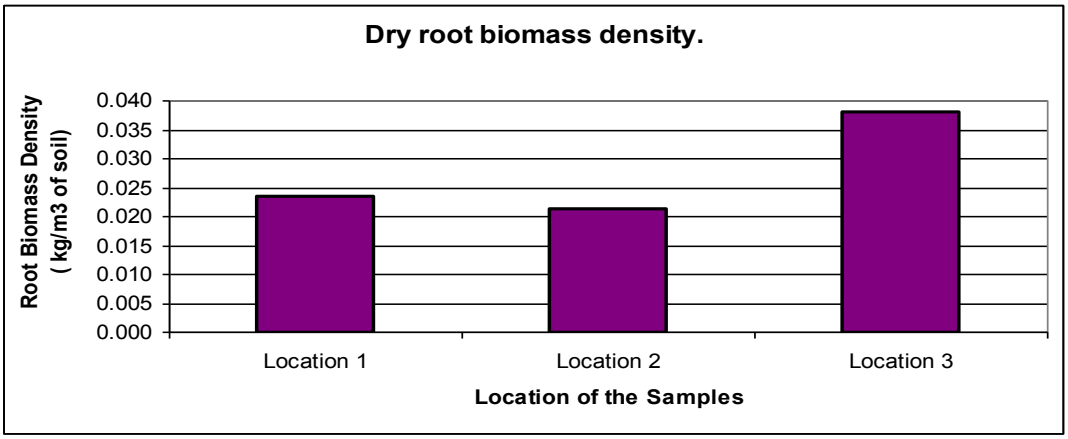


**Figure 12: Dry root biomass density.**

Figure 12 showed that the highest biomass density indicated from samples at location 3. The other two locations showed slightly different value of 9.4% in biomass density. Samples from location 2 gave the lowest value of biomass density resulted in lowest shear strength values.

## C. Moisture Content and Particle Size Distribution

Shear stress is calculated as a function of both vegetal and soil resistance. Vegetal resistance of the soil/plant boundary is calculated as a function of both components including roots density, and soil resistance as a factor of grain size. Vegetal and soil parameters are combined to form the total shear stress resistance of the soil/plant boundary. The soil tests performed in this study were particle size distribution and water content. These two tests seem to be very essential in order to relate soil condition and environment with the growth pattern of the roots. At the location of typical soil 3, samples of soil were taken at 1 m radius. It is easy to get the samples from this location because the place was bare and no roots of vegetation in the soil blocks. The roots might affect the results of the test performed. The soil at the site consisted of a poorly cohesive sand which might be derived from the floodplain sediments. The water content indicated also varies with the location of the samples. Sample 3 (M56) gave the highest moisture content; 14.1% followed by sample 1, M52 and sample 2, M54. Even though the samples come from the same type of soil, the moisture content seemed to be different.

## DISCUSSION

### A. Soil-plant Shear strength

The graphs of shear stresses versus displacements show that, in general, the shear stresses were still increasing at the end of the tests. This clearly indicates that root tensile failure did not occur during the shear tests. Root elongation or slippage rather than breakage was the most common condition during failure. This mode of failure was evident in examination of the samples after the testing was completed and has been observed by other investigators studying the effects of fibrous inclusions on non-cohesive soils. The steadily increase of shearing resistance of all samples from location 1, 2 and 3 also show that shear stress within the soil was transferred to the.

Survival and development of plants after a partial failure can readily allow vegetation to provide continued and renewed reinforcement of soils, and also to, in effect, re-compact soils due to matrix suction effects. These roles allow vegetation to limit and manage the amount of ongoing loss and damage that may occur due to experience of some slope failure, unlike fallow soils which remain vulnerable to ongoing mass wasting due to low residual strengths. The shear stresses obtained in each plant species show a very wide spread, making it difficult to come to reasonable conclusions without a suitable statistical analysis. This degree of variation is illustrated, for example, in sample 1 and sample 2 in Figure 8 and 9 or sample 1 and sample 3 in Figure 10. This wide variation is also noted for the un-vegetated soil blocks, 7.

**Table 1: Average shear stress at particular Displacement**

| | **Average shear stress at particular displacement (kPa)** | | | |
|---|---|---|---|---|
| **Location / Displacement (mm)** | ***Unvegetated soil*** | ***Location 1*** | ***Location 2*** | ***Location 3*** |
| **4** | 13.6 | 15.3 | 14.2 | 13.5 |
| **6** | 15.4 | 18.2 | 17.3 | 17.1 |
| **8** | 17.1 | 21.4 | 20.2 | 20.5 |
| **10.8** | 18.7 | 25.1 | 23.9 | 23.9 |
| **11.8** | 18.8 | 26.2 | 25.3 | 25.4 |
| **12.8** | 19.0 | 27.3 | 27.0 | 26.9 |
| **13.3** | 19.1 | 27.4 | 27.2 | 27.3 |

*Bermuda grass* roots in this sandy soil had large reinforcing effect, where the ultimate shear resistance obtained in samples from location 2 and 3 followed in decreasing order by samples from location1. *Bermuda grass* roots increased soil shear resistance by 27.3 kPa compared to 19.1 kPa for un-vegetated soil at a displacement of 13.3 cm (location 3). The relative strength increase at the same displacement (13.3 cm) was 43.5% for location 1 and 42.4% for location 2.

The increment of soil strength caused by the roots also had been proven by other researcher before (Abenneth and Rutherfud) [28] where small increase in root density increases the soil shear strength. It was found that the traction effect of the roots increased the tensile strength of the shallow rooted soil by 4.2~5.6 kPa. This finding was true for the samples of soil blocks from location 2 and 3 at displacement 10.8 mm. From this study, the general range of shear strength increment was 0.6 – 8.3 kPa.

Table 1 shows that the shear stresses of the soils permeated with the grass roots at location 1,2 and 3 are significantly different from the un-vegetated condition. Whereas, the shear stresses of soils from location 3 at displacement 4 cm are not significantly different from the un-vegetated (Figure 11).. These root cohesion values are conservative, because they were determined from a shear displacement of 4 cm and not from the peak stresses, which were never reached during these tests. At the surface, this investigation reveals an obvious relationship between soil shear strength and plants, although statistical analysis dictates that no sweeping conclusions be drawn. Nevertheless, the nature of the conditions, the testing procedure, and the analytical approach are conservative, so it is reasonable to state that the actual role of plants is larger than documented, and that the variability between specimens contributed to the lower degree of statistical validation of the results.

**B. Root biomass density**

Root biomass density is proportional to the shear strength increase [29]. However, this is true for the plants which have same morphology. As grasses grow, their contribution to a site's stability increases as a function of the speed and ease at which roots "colonise" the soil. This depends on the root content, the roots' material properties, and the morphology or architecture. Root morphology and architecture may be genetically controlled or modified by environmental and adaptation factors. The variation in root biomass can be affected by the variation of the water content. The water content is not constant at different location. This showed how the environment condition can change the value of the root density. As water flows to the soil, mass of adsorbed water formed around the particles. As the water film increases, the particles of the soil can be packed more closely when it is more lubricated. However the pore water pressure in the adsorbed films tends to push the particles apart and so increase the water content.

Strength of roots is also influenced by roots size which is highly dependent on the root density and activity of decay organism. In sandy soil, the moisture movement can move some fine particles. Scouring is the removal of material by surface water. Different density will give different value of root size. In this study all the roots determined were less than 2 cm which proved the theory by Coppin and Richard where the soil cohesion is limited to the roots up to 2 cm in diameter [4].

It is noted that although samples from location 3 had the highest root biomass density, its average maximum shear strength was smaller than location 1. In fact its shear strength was the smallest one at displacement 4cm, 6 cm and 12.8 cm. This might indicate that the tensile strength of the roots is smaller than those other roots from other locations although it comes from same species of grass or its root surface friction is lower, hence allowing slippage. However, several other factors such as root orientation, for example, could be the cause for having small shear strength with relatively high root biomass. Figures 12 shows typical shear stress and root biomass density. The species tested showed a fairly well defined shear plane upon failure, with most roots not broken at or near this plane but elongated at increasing strength. Whereas the species at location 1 showed a wider shear zone with numerous roots extending through and beyond this deformed shear zone, they exhibited some stretching and pullout from the adjoining soil matrix.

The relationship between soil condition and root architecture is needed to be taken to consideration. Root architecture relates to the growth pattern which is greatly dependent on the moisture level. The site conditions also influence the rooting habit and growth. The root growth can be analyzed by determining the roots density relying on the biomass as more accurate indicator. The root biomass density was different at each location. Although the soil is considered to be of the same sandy soil, the water contents were different. The result of the water content showed that different locations had different moisture contents. This showed that the growth pattern can be affected differently by the hydrological condition.

Finally, the age of the roots itself can influence the strength and reinforcement of the roots system. The grass was estimated to be 2.5 years old. The root geometry can be limited due to the time from the vegetation grows. The older the vegetations, the denser it will be [30]. Wide variety of the vegetation is influenced by the age of the vegetation.

## CONCLUSION

This investigation generated data about the contribution of selected native plant species (*Bermuda grass*) roots to soil shear strength. These data can be used to perform qualitative or semi-quantitative assessment of vegetated slopes or slope stability analyses. Soil block samples permeated with roots of plant species that are commonly used in remediation and habitat restoration purposes were tested in a large direct shear apparatus. Shear stress results of rooted soils were compared with results of un-vegetated soil blocks with similar soil types. Un-vegetated soil blocks reached an average maximum force at a displacement of 11.8 cm, 12.3 cm and 13.3 cm. This displacement was used as the ultimate shear stress for the un-vegetated soil. The shear stresses for the root permeated soil blocks were compared to this stress in order to assess the stress increase due to the plant roots. Samples from location 2 and 3 had the largest increase in shear stress, reaching a value of 32.2 kPa at a displacement of 13.3 cm. The maximum shear stress for the un-vegetated soil was just 19.1 kPa at the same displacement. Hence, the root systems of these plants resulted in an increase of strength as compared with fallow soils.

**The conclusions from this study are the following:**

- The shear stress increase caused by the root system of these plants is significantly different from the shear stress of the un-vegetated treatment. The shear stresses in most of the rooted blocks were still increasing at the end of the test (maximum displacement of about 15 cm), indicating that root tensile failure did not occur during the shear tests.
- Additionally, the mode of failure appears to allow for the survival of the herb, and possibly certain woody, species after the event. In general, the shear stress results were very widespread because of the uncontrolled conditions of the natural site conditions of the samples. It is evident that plant roots provide a substantial increase in the shear strength of soils.
- On average, all samples rooted by grass, had a shear stress that was statistically different from un-vegetated fallow soil conditions. The values of soil mass shear strength and root biomass depend on more environmental variables shown by the variation in the moisture content.
- The results and findings from this study are true for the site condition which had inconsistent values of water content. The sandy soil with variation in moisture level tends to give different values of soil-root strength. These show how the relationship between soil and environmental condition can affect the growth of the roots which directly influences the soil-root strength.

## REFERENCES

[1] Gray, D.H. and R.B. Sotir. Biotechnical and Soil Bioengineering Soil Stabilisation: A Practical guide for Erosion Control, Wiley, New York, 1996

[2] Vidal, H. The Principles of Reinforced earth. Highway Research Record No. 282. pp. 1-16, 1969.

[3] Gray, D.H. and A.T. Leiser. Biotechnical Slope Protection and Erosion Control. Van Nostrand Co.
NY. 1982.

[4] Coppin, N.J. and Richards, I.G. Use of Vegetation in Civil Engineering. Butterworths. London, 1990

[5] Burroughs, E.R. and Thomas, B.R. Declining Root Strengths in Douglas-Fir after Falling as A Factor in Slope Stability. Research Paper INT-190, 27 pp. Forest Service, I.S. Dept. of
Agriculture, Ogden, Utahm 1977

[6] O'Loughlin, C.L. and Watson, A. Root-wood strength deterioration in *radiate pine* after clear felling, New Zealand Journal of Forest Science, 9(3): 284-293, 1979

[7] Swanston, D.N. and Dryness, C.T. Stability of Steepland. Journal of Forestry. 71(5):246-269 1973

[8] Riestenberg, M.M. Anchoring of thin colluviums by Roots of *Sugar Maple and White Ash* on Hillslopes in Cincinnati. U.S. Geological Survey Bulletin 2059-E. 1994

[9] Hewitt, J.S. and A.R. Dexter. The behaviour of Roots encountering cracks in soil: Development of a Predictive Model, Plant and Soil. 79: 11-28, 1979

[10] Tardieu, F. Analysis of the Spatial Variability of maize root density. Plant and Soil. 107: 259-266., 1988

[11] Lungley, D.R.,The Growth of Root Systems – A numerical Computer Simulation Model. Plant and Soil. 38: 145-159, 1973

[12] Henderson, R., Ford, E.D. and E. Renshaw. Morphology of the Structural Root System of
*Sitka Spruce* and Computer Simulation of Rooting Patterns. Forestry. 56: 121-135, 1983

[13] Rose, D.A.The Descript ion of the Growth of Root Systems. Plant and Soil. 75: 405-415. 1983.

[14] Diggle, A.J. ROOTMAP – a model in three dimensional coordinates of the Growth and Structure of Fibrous root system, Plant and soil, 105: 169-178. 1988.

[15] Pages, L. Jordan, M.O. and Picard, D. A simulation model of the three dimensional Architecture of the maize root system. Plant and Soil. 199: 147-154., 1989

[16] Zimmer, W.J. and Grose, R.J. Root Systems and root/shoot Ratios of Seedlings of some *Victorian Eucalyptus*. Australian Forestry. 22(2): 13-18., 1958

[17] Ashton, D.H. The Root and Shoot Development of *Eucalyptus regnans F. Meull*. Australian
Journal of Botany, 23: 867-887., 1975

[18] Dabral, B.G., Pant, S.P. and Pharasi, S.C. Root Habits of *Eucalyptus*: Some Observation. Indian Forester. 113(1): 11-32., 1987

[19] Stone, E.L. and Kalisz, P.J. On the maximum extent of tree roots. Forest Ecology and Management. 46: 59-102. 1991

[20] Todd R.H. and E.M. Payson,The use of Vegetation in Bioengineered Stream banks: Shear Stress Resistance of Vegetal Treatments. ASCE 1998

[21] Schiechtl, H.M. Bioengineering for Land Reclamation and Conservation. University of Alberta Press, Edmonton, Canada, 1980

[22] Greenway, D.R. 1987. Vegetation and Slope Stability: In Slope Stability. Eds: M.G. Anderson and K.S. Richards. John Wiley & Sons Ltd, Chichester, pp. 187-230, 1987

[23] Marden, M. and Rowan, D. 1. Protective value of vegetation on tertiary terrain. New Zealand Journal of Forestry Science 2393): 255-263. 1993.

[24] Phillips, C.J. and Watson, A.J. Structural tree root research in New Zealand. Landcare Research Science Series No. 7. Manaaki Whenua Press. 71p. 1994.

[25] Waldron, L.J. The Shear Resistance of root-permeated homogenous and stratified soil, Soil Science Society of America Journal, 1977

[26] Wu, T.H. and Watson, A. In-situ Shear Tests of Soil Blocks with Roots. Can. Geotech. Journal 35: 579-590, 1998

[27] Shewbridge, E.S. and S. Nicholas, Formation of Shear Zones in Reinforced Sand, Journal of Geotechnical Engineering, 122(11) November 1996

[28] Abernethy, B. and Rutherfurd, I.D. The Distribution and Strength of Riparian Tree Roots in relation to riverbank reinforcement. Hydrological Processes, 15(1): 63-79.2001

[29] Ziemer, R.R. 1981. Roots and the Stability of Forested Slopes. Publication, No. 132. International Association of Hydrologic Sciences, pp. 343-361.

[30] Schiechtl, H.M., Bioengineering for Land Reclamation, Alberta Press, 404 p, 1980.